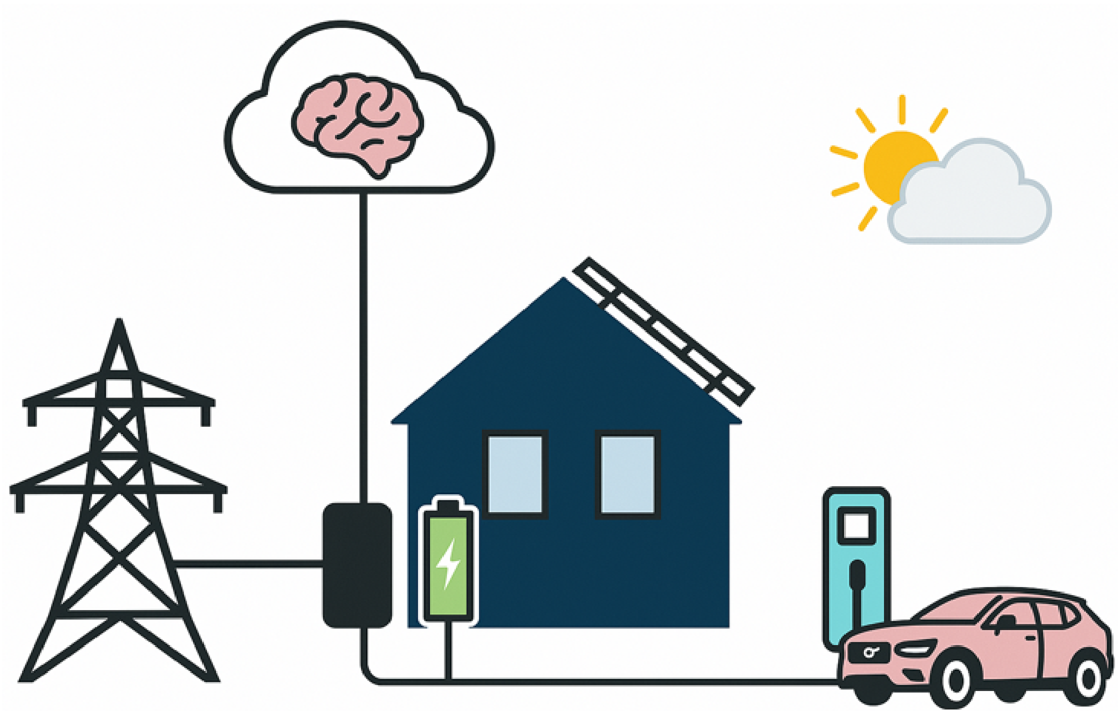

Home Energy Management System Optimization with Stochastic Programming

Home Energy Management System Optimization for Residential Homes with Vehicle to Everything Battery Electric Vehicles

Master's thesis in Engineering Mathematics and Computational Science

Jessica El-Jabaoui, Edvin Sand

DEPARTMENT OF MATHEMATICS AND STATISTICS

CHALMERS UNIVERSITY OF TECHNOLOGY

Gothenburg, Sweden 2025

www.chalmers.se

Master Thesis 2025

Home Energy Management System Optimization with Stochastic Programming

Home Energy Management System Optimization for Residential Homes with Vehicle to Everything Battery Electric Vehicles

Jessica El-Jabaoui, Edvin Sand

Department of Mathematics
Applied Mathematics and Statistics
Chalmers University of Technology
Gothenburg, Sweden 2025

Home Energy Management System Optimization with Stochastic Programming
Home Energy Management System Optimization for
Residential Homes with Vehicle to Everything Battery Electric Vehicles
Jessica El-Jabaoui, Edvin Sand

Industrial Supervisor: Viktor Larsson, Volvo Car Corporation
Examiner and Academic Supervisor: Larisa Beilina, Applied Mathematics and Statistics

Master's Thesis 2025
Department of Mathematics
Division of Applied Mathematics and Statistics
Chalmers University of Technology and Gothenburg University
SE-412 96 Gothenburg
Telephone +46 31 772 1000

Cover: Visualization constructed by Jessica El-Jabaoui and Edvin Sand of a HEMS.

Typeset in LaTeX
Printed by Chalmers Reproservice
Gothenburg, Sweden 2025

Home Energy Management System Optimization with Stochastic Programming
Home Energy Management System Optimization for
Residential Homes with Vehicle to Everything Battery Electric Vehicles
Jessica El-Jabaoui, Edvin Sand
Department of Mathematics
Division of Applied Mathematics and Statistics
Chalmers University of Technology and Gothenburg University

Abstract

This thesis explores the optimization of Home Energy Management Systems (HEMS) with a focus on battery electric vehicle (BEV) charging, using two different methods: Linear Programming (LP) and Stochastic Programming. The BEV is modeled with vehicle-to-everything (V2X) functionality, allowing it to both charge and discharge energy to support the household or grid.

The primary aim is to incorporate uncertainty into the optimization process, acknowledging that in real-world scenarios, exact information about the vehicle's arrival time and current state of energy (SOE) is rarely known in advance. We begin by examining uncertainty in both arrival time and SOE, then narrow the focus to uncertainty in SOE alone. In the final part of the thesis, we investigate the impact of power tariffs to determine whether incorporating them into the optimization yields meaningful benefits for households.

Our results show that stochastic optimization introduces a small increase in computational cost while significantly reducing the risk of unwanted outcomes caused by uncertainty. While the cost difference per vehicle is fractional, the impact becomes substantial when scaled across many BEVs. The benefits extend beyond cost savings, by optimizing charging to occur during low spot price hours, we also reduce the environmental footprint, as electricity is typically greener during these periods. In addition, the ability to sell back energy to the grid when it is not needed helps balance demand and supports grid stability.

Therefore, assuming perfect foresight and relying solely on LP is not representative of real-world conditions. We conclude that accounting for uncertainty through stochastic methods is a cost-effective and scalable improvement for future energy management systems.

Keywords: Home Energy Management System, Deterministic Equivalent of a Stochastic Problem (DESP), Linear Programming, Battery Electric Vehicle, Vehicle-to-Grid, Uncertainty Modeling, Demand-Charge Tariffs, Demand Response, Smart Charging, Energy Flexibility.

Acknowledgements

We would like to thank Viktor Larsson, our supervisor at Volvo Cars, for his continuous support throughout this thesis. His willingness to discuss, explain, and guide us. We are also grateful to his colleagues who offered their expertise when needed, Niklas Åkerblom and Magnus Eldén. We also wish to extend our thanks to our examiner and academic supervisor, Larisa Beilina, for her guidance and support throughout the spring.

Jessica El-Jabaoui and Edvin Sand, Gothenburg, May 2025

List of Acronyms

Below is the list of acronyms that have been used throughout this thesis listed in alphabetical order:

BEV	Battery Electric Vehicle
BPSO	Binary Particle Swarm Optimization
DCT	Demand-Charge Tariff
DESP	Deterministic Equivalent Stochastic Problem
EV	Electric Vehicle
HEMS	Home Energy Management System
LP	Linear Programming
MILP	Mixed Integer Linear Programming
ODE	Ordinary Differential Equation
PV	Photovoltaic
RESS	Residential Energy Storage System
RTP	Real-time Pricing
SOE	State of Energy
SP	Stochastic Programming
s.t.	Subject to
V2G	Vehicle-to-Grid
V2X	Vehicle-to-Everything

Nomenclature

Below is the nomenclature of indices, sets, parameters, and variables that have been used throughout this thesis.

Indices

b	Index for battery type
B	Index for the BEV battery
c, d	Indices for charge and discharge variables
i	Index for decision variables
k	Index used to map matrix elements to their corresponding positions in a vectorized representation
R	Index for the RESS battery
s	Index for scenarios
t	Index for time step
buy, $sell$	Indices for buying and selling power
$home$	Index referring to household power consumption
$solar$	Index for power flows related to solar generation
sol	Index for parameters in the solar panel model
sun	Index referring to solar irradiance
$base$, $heat$, $cool$	Indices related to components of total household power consumption

Sets

$\mathcal{B}$	Set of batteries
$\mathcal{S}$	Set of scenarios

Parameters

a_{sol}	Surface area of solar panels (m^2)
E_b	Maximum capacity of battery b (kWh)
$Initial^B_{SOE}$	Initial SOE for the BEV (%)
N_A	Number of elements in constraint matrix A
N_{sol}	Number of solar panels
P^n_{sol}	Rated power for each solar panel (kW)
$\mathcal{T}$	Number of time steps
t_{in}	Plug-in time for the BEV
t_{out}	Plug-out time for the BEV
$Target^B_{SOE}$	Target SOE for the BEV (%)
$Target^R_{SOE}$	Target SOE for the RESS (%)
u_1, u_2	Number of decision variables in stage 1 and 2 respectively
γ_{cf}	Capacity factor
δ	Loss during energy conversion
η_{sol}	Solar panel conversion efficiency

Variables

$c_{buy}(t)$, $c_{sell}(t)$	Cost of buying and selling electricity (SEK/kW)
$P_{solar}(t)$	Power generated by solar panels (kW)
$P_{home}(t)$	Total household power demand (kW)
$P_{base}(t)$, $P_{heat}(T_{amb}(t))$, $P_{cool}(T_{amb}(t))$	Components of household power demand (kW)
$P_{buy}(t)$, $P_{sell}(t)$	Power bought or sold from the grid (kW)
$P_{dB}(t)$, $P_{cB}(t)$	Discharge/charge power of BEV (kW)
$P_{dR}(t)$, $P_{cR}(t)$	Discharge/charge power of RESS (kW)
$SOE_B(t)$, $SOE_R(t)$	State of energy of BEV and RESS (%)
$T_{amb}(t)$	Ambient temperature (°C)
$I_{sun}(t)$	Solar irradiance (W/m^2)

Contents

List of Acronyms **ix**

Nomenclature **xi**

List of Figures **xvii**

List of Tables **xxi**

1 Introduction **1**
1.1 Background 1
1.2 Problem formulation 1
1.3 Aim 3
1.4 Research Questions 3
1.5 Assumptions and Limitations of the Problem 4
1.6 Contribution 5
1.7 Outline 5

2 Home Energy Management System Overview **7**
2.1 Details of the HEMS 7
2.2 System Model 8
2.2.1 Solar Panel Model 8
2.2.2 House Model 9
2.2.3 RESS Model 10
2.2.4 BEV Model 10
2.2.5 Energy Meter Model 11
2.2.6 Electricity Price Model 11

3 Previous Work **13**
3.1 HEMS Optimization 13
3.1.1 Mathematical Techniques 13
3.1.2 Heuristic Techniques 14
3.2 Mixed Integer, known BEV arrival time 14
3.3 Stochastic Programming 14
3.4 Mixed Integer, Stochastic driving schedule 15
3.5 Meta-Heuristic Optimization Methods 15
3.6 Electricity Price Models, with Demand Charge Tariffs, without BEV 15
3.7 Previous Work Summary 16

4 Theory **17**
4.1 Linear programming 17
4.2 Stochastic programming 17
4.2.1 Two-stage Stochastic Programming 17
4.2.2 Scenario-based approach 18
4.2.3 Deterministic equivalent stochastic programming 19
4.3 Demand-Charge Tariffs 20

5 Implementation **23**
5.1 Mathematical Implementation 23
5.1.1 Linear Problem Formulation 23
5.1.1.1 Linearization of the Battery Models 23
5.1.1.2 Decision variables 24
5.1.1.3 Cost 25
5.1.1.4 Objective function and LP problem 25
5.1.2 Deterministic Equivalent Stochastic Problem 27
5.1.2.1 Uncertainty in arrival State of Energy 28
5.1.2.2 Illustrative Example: Two Scenarios 30
5.1.2.3 Memory storage of different scenarios 32
5.2 Demand-Charge Tariffs 32
5.3 Algorithm 33
5.4 Assumptions in the Implementation 34
5.4.1 Home 35
5.4.1.1 Household energy demand 35
5.4.2 Batteries (BEV and RESS) 35
5.4.2.1 SOE and time of arrival 35
5.4.3 Electricity prices 35
5.4.4 Weather 36
5.5 Non feasible solutions 36

6 Results and Discussion **37**
6.1 Baseline Linear Programming Implementation 39
6.2 Cost Sensitivity to BEV Arrival Time in a LP Setting (w/o Tariffs) . 40
6.3 Uncertainty in BEV Arrival SOE 44
6.3.1 Visualization of DESP Results 44
6.3.1.1 BEV/RESS Trajectories DESP 44
6.3.1.2 Battery System Configuration Comparisons 48
6.4 Case study 51
6.4.1 Extreme days 52
6.4.2 Stochastic vs wrong assumption 53
6.4.2.1 Stochastic vs wrong assumption with the most extreme days - winter 54
6.4.2.2 Stochastic vs wrong assumption with the most extreme days - summer 55
6.4.2.3 Stochastic vs wrong assumption with random days . 56
6.5 Demand-Charge Tariffs 57
6.5.1 BEV/RESS Trajectories with Demand-Charge Tariffs 57

6.5.2 Electricity from the grid 62
6.5.3 Tariff Cost Comparison 65

7 Conclusion & future research 67
7.1 Conclusion 67
7.1.1 Research Questions 67
7.2 Future Research 69
7.2.1 Extended Optimization Horizon 69
7.2.2 Additional Scenarios 69
7.2.3 Handling of Non-feasible Solutions 70
7.2.4 Demand-Charge Tariffs 70
7.2.5 Additional Future research 71

Bibliography 73

A Appendix I
A.1 Additional Implementations: I
A.1.1 Uncertainty in Electricity Price I
A.2 Additional Results: III
A.2.1 BEV arrival time in a LP setting III
A.2.2 RESS/BEV Trajectories for three scenarios III

List of Figures

1.1 Illustration of the HEMS setup 2

2.1 Example of the solar production ($P_{solar}(t)$) over 24 hours, starting 07:00 January 5th 2024. 9
2.2 Example of the Home Load ($P_{home}(t)$) over 24 hours, starting 07:00 January 5th 2024. 10
2.3 Example of spot prices for buying and selling electricity over 24 hours, starting 07:00 January 5th 2024. 12

4.1 Two-stage SP problem represented by a scenario tree [1]. 19

6.1 Optimized charging trajectories of the BEV and RESS for a single day, with the BEV arriving at 16:00 with 50% SoE and leaving at 7.00 with target SoE of 90%. 39
6.2 Cost differences for various BEV arrival times on one winter (5 Jan 2024) and one summer day (1 Jul 2024) for a typical current battery system. Initial SOE 50%, target SOE 90%. 40
6.3 Cost differences for various BEV arrival times on one winter (5 Jan 2024) and one summer (1 Jul 2024) day for Future Battery System A. Initial SOE 50%, target SOE 90%. 41
6.4 Cost differences for various BEV arrival times on one winter and one summer day for Future Battery System B. Initial SOE 50%, target SOE 90%. 42
6.5 Cost differences for various BEV arrival times on 100 winter days (fr. 1 Dec 2023) and 100 summer days (fr. May 2024) for a typical current battery system. Initial SOE 50%, target SOE 90% each day. 43
6.6 Cost differences for various BEV arrival times on 100 winter days (fr. 1 Dec 2023) and 100 summer days (fr. 1 May 2024) for Future battery system B. Initial SOE 50%, target SOE 90% each day. 43
6.7 SOE trajectories of both the RESS and BEV on a winter day (5 Jan 2024) under two BEV arrival SoE scenarios. 45
6.8 SOE trajectories of both the RESS and BEV on a summer day (1 Jul 2024) under two BEV arrival SoE scenarios. 47
6.9 SOE trajectories of the RESS and BEV for a winter day (5 Jan 2024) under Future System A (50 kWh), with two different BEV arrival SoE scenarios. 49

6.10 SOE trajectories of the RESS and BEV for a winter day (5 Jan 2024) under Future System B (100 kWh), with two BEV arrival SoE scenarios. 50
6.11 Costs LP 2 scenarios and LP wrong assumption over 5 winter month. 52
6.12 Cost stochastic method vs LP wrong assumption with only 20% wrong assumption (extreme days) over 5 winter month (November-Mars). 54
6.13 Cost stochastic method vs LP wrong assumption with only 20% wrong assumption (extreme days) over 5 summer month (May-Sep) . 55
6.14 Cost stochastic method vs LP wrong assumption with only 20% wrong assumption (random days) over 5 winter month. Average of 20 runs 56
6.15 Linear optimization for a 20 kWh battery comparing low-tariff and no-tariff scenarios, with the BEV trajectory on the right and the RESS trajectory on the left. 57
6.16 Linear optimization for a 50 kWh battery comparing low-tariff and no-tariff scenarios, with the BEV trajectory on the right and the RESS trajectory left. 58
6.17 Linear optimization for a 20 kWh battery comparing high-tariff and no-tariff scenarios, with the BEV trajectory on the right and the RESS trajectory on the left. 58
6.18 Linear optimization for a 50 kWh battery comparing high-tariff and no-tariff scenarios, with the BEV trajectory on the right and the RESS trajectory on the left. 59
6.19 Stochastic optimization for a 20 kWh battery comparing low-tariff and no-tariff scenarios, with the BEV trajectory on the right and the RESS trajectory on the left. 60
6.20 Stochastic optimization for a 50 kWh battery comparing low-tariff and no-tariff scenarios, with the BEV trajectory on the right and the RESS trajectory on the left. 60
6.21 Stochastic optimization for a 20 kWh battery comparing high-tariff and no-tariff scenarios, with the BEV trajectory on the right and the RESS trajectory on the left. 61
6.22 Stochastic optimization for a 50 kWh battery comparing high-tariff and no-tariff scenarios, with the BEV trajectory on the right and the RESS trajectory on the left. 61
6.23 Electricity purchased from the grid over one day under stochastic optimization without tariffs vs with low tariffs, using a 20 kWh RESS 62
6.24 Electricity purchased from the grid over one day under stochastic optimization without tariffs vs with high tariffs, using a 20 kWh RESS 63
6.25 Electricity purchased from the grid over one day under stochastic optimization without tariffs vs with low tariffs, using a 50 kWh RESS 63
6.26 Electricity purchased from the grid over one day under stochastic optimization without tariffs vs with high tariffs, using a 50 kWh RESS 64
6.27 Total System Cost Comparison: Integrated low Tariff Optimization vs. Post-hoc low Tariff Application over 5 winter month 65

A.1 Cost differences for various BEV arrival times on 100 winter days and 100 summer days for Future battery system A. III
A.2 SOE trajectories of the BEV on a winter day, with Future System B (100 kW). The BEV arrives at 18:00, with three possible scenarios. . III
A.3 SOE trajectories of the RESS and corresponding cost comparison for a winter day, using Future System B (100 kW). The BEV arrives at 18:00, with 3 possible scenarios. IV
A.4 SOE trajectories of the BEV on a winter day, with Future System A (50 kW). The BEV arrives at 14:00, with three possible scenarios. . . . IV
A.5 SOE trajectories of the RESS and corresponding cost comparison for a winter day, using Future System A (50 kW). The BEV arrives at 14:00, with 3 possible scenarios. V

List of Tables

2.1 Summary of HEMS system specifications and input data 8

5.1 Memory storage depending on size of matrix A 32

6.1 Top 10 days with the largest recorded differences, winter. 53
6.2 Top 10 days with the largest recorded differences, summer. 53

1
Introduction

1.1 Background

The transition to a more sustainable energy system is driving a growing number of households to adopt technologies such as battery electric vehicles (BEVs), rooftop solar panels, and residential energy storage systems (RESS). This development presents a valuable opportunity for improving how energy is consumed, stored, and exchanged within the home. A Home Energy Management System (HEMS) is a key component in this shift; by intelligently scheduling the charging and discharging of BEVs and RESSs, such a system can help reduce electricity costs and make better use of renewable energy.

RESS enables users to store excess solar power produced during the day and use it later during peak-price hours when solar production may be lower. This reduces reliance on grid energy during expensive periods and can also serve as a backup power source during outages. For BEVs, smart charging strategies can align electricity use with low-price periods, further improving cost efficiency.

Beyond individual cost savings, HEMS optimization supports broader sustainability goals. By flattening household load profiles and shifting consumption away from peak hours, these systems can help reduce strain on the electricity grid, especially during high-demand periods such as cold winter evenings. This in turn reduces stress on the electricity grid during periods of high demand and supports a more balanced and resilient energy system.

In this context, optimizing the operation of HEMS as well as taking into account time-varying electricity prices, solar generation, user behavior, and system constraints, is both timely and relevant. This thesis explores such optimization strategies with a particular focus on the interaction between BEVs, RESS, and the grid, under both deterministic and uncertain conditions.

1.2 Problem formulation

The energy management system we are interested in is a HEMS that helps households optimize their energy use, storage and buying/selling of electricity.

An illustration of the HEMS setup can be seen in the Figure 1.1.

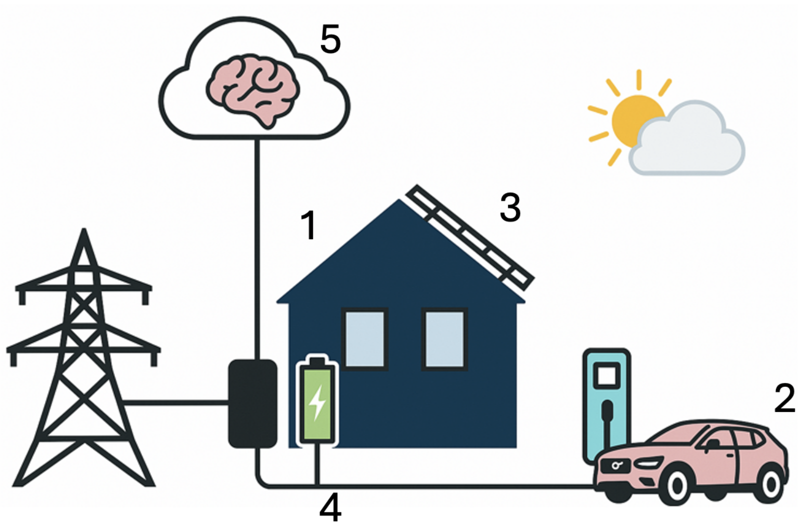

Figure 1.1: Illustration of the HEMS setup

The system consists of the following components:
1. The house (as the primary point of energy consumption)
2. A battery electric vehicle (BEV)
3. Solar panels
4. A home battery (residential energy storage system, RESS)
5. A real-time electricity meter

The goal is to reduce total energy costs for the households by making smart decisions about when to use, buy/sell or store electrical energy. The system should also be able to help reduce peak loads, contributing to a more stable and balanced energy consumption while staying user friendly, ensuring that energy savings does not come at the cost of everyday comfort and usability for the household.

The optimization model aims to minimize the total electricity cost of a household energy system, subject to a set of operational and physical constraints. These include limitations of energy system components such as RESSs, BEVs, and solar panels, as well as the need to satisfy household electricity demand and ensure feasible energy exchange with the grid. Conceptually, the problem can be expressed as

$$\begin{aligned} \min \quad & \text{Electricity cost} \\ \text{s.t.} \quad & \text{Component constraints (e.g. BEV, RESS)} \\ & \text{Demand fulfillment (e.g. household, BEV charging)} \\ & \text{Power and energy flow limits} \end{aligned} \tag{1.1}$$

A straightforward approach for solving this problem is to assume that all parameters, such as electricity prices, energy demand, and vehicle usage, are known with certainty. This leads to a deterministic optimization problem, which is computationally efficient and easy to implement. However, this assumption often fails to reflect the uncertain nature of real-world energy systems. With this in mind, the goal of this work is to develop a formulation that accounts for key uncertainties while maintaining computational tractability and scalability.

1.3 Aim

The aim of this thesis project is to study HEMS by extending previous research performed at Volvo Car Corporation where the problem has been formulated as a linear programming (LP) problem, where all input parameters have been assumed to be known. The goal is to improve the model such that it more accurately reflects real-world conditions where parameter values are uncertain. The project has focused on developing a framework with two main parts:

i) **Supervisory Level:** For situations when there is no live information about the BEV, such as when it will arrive or how much charge it has. The system needs to work with limited information and uncertainty to decide how to operate.

ii) **Real-Time Updates:** In this part, the system will use new information as it becomes available. It will adjust and optimize its decisions based on this updated data.

This approach aims to make the HEMS more effective and reliable in managing energy under uncertainties.

1.4 Research Questions

To achieve our aim, we have a few research questions we have formulated:

- Given an uncertainty, how does the formulation of the HEMS optimization problem change?

- Is it possible to get a lower energy cost with another optimiation method than LP, such as stochastic optimization?

- How sensitive is the optimal solution of a deterministic LP-problem to uncertainties in the variables?

  - *Does an uncertainty in the variables, e.g., time of arrival and difference in the cars state of energy, have an impact on the optimal solution?*

  - *With the uncertain variables, how will the charge/discharge energy trajectories change for the BEV and RESS?*

- How do demand-charge tariffs influence the charging trajectories of the BEV and RESS, and is it beneficial to include them in the optimization?

1.5 Assumptions and Limitations of the Problem

Previous work conducted by Volvo Car Corporation have formulated the problem as an LP-problem. To do this, certain assumptions and simplifications have been necessary. This study will reuse the same assumptions and simplifications for the HEMS component and the electricity price models.

One of the key assumptions concerns the prediction accuracy, particularly regarding weather forecasts. It is assumed that the 24-hour weather forecast is accurate. This assumption enables the computation of energy requirements for heating or cooling, as well as the energy generated by solar panels.

Simplifications are also necessary to linearize the problem. These include the use of simplified linear models for external factors and disturbances that the HEMS system cannot control. For example, home energy consumption is modeled as a linear function of the hourly ambient temperature.

A car can either be "awake" or "asleep" between charging sessions. When the car is charging, there is a standby cost associated with being "awake". Conversely, if the car is not charging, it can be completely turned off, eliminating such costs. In this study, however, it is assumed that the car remains "awake" and constantly available at all times. Any standby cost or energy consumption related to this state is disregarded. Furthermore, this study also neglects wear and tear on the RESS and the BEV due to temperature variations and discharge cycles.

To clarify the assumptions and simplifications used in this study, they are summarized in the list below:

- Weather Forecasts are accurate 24 hours ahead of time. Key inputs of the modeled home consumption and solar generation is known (e.g., ambient temperature and solar irradiance).
- No information is available about the car's status when it is away from home, i.e. the vehicle arrival time and energy level is not updated when it is away from home.
- All BEVs are assumed to be compatible with vehicle-to-grid (V2G) or vehicle-to-everything (V2X) technology.
- Linear models of components are assumed to enable formulation as an LP problem.
- The BEV is assumed to be "awake" at all times to avoid a mixed integer problem with "awake" and "asleep" states. Any costs associated with this state is disregarded.

- Wear and tear of the RESS and BEV is not considered.

These assumptions result in simplifications of the HEMS scheduling problem to focus the scope of this thesis on comparing optimization methods rather than including every technical detail. Our work lays a foundation for these methods that can be extended in future research or added later in a real-world version of the system.

1.6 Contribution

This work provides insights into how uncertainty in real-life conditions, such as vehicle arrival time and state of energy, can impact energy optimization outcomes. It also explores the potential influence of demand-charge tariffs on charging behavior. The main contribution of this thesis is the formulation of the HEMS control problem as a stochastic linear programming problem using a scenario-based approach. The findings aim to support the development of smarter and more realistic optimization strategies, which in the future could help BEV owners reduce costs, support the grid, and increase the use of greener electricity.

1.7 Outline

The thesis is structured into six main sections, each building on the previous to provide a clear understanding of the research. Upcoming chapters begin with an introduction to the HEMS, outlining all components and presenting the complete system model. Chapter 3 reviews earlier studies, focusing on the mathematical techniques used to solve similar optimization problems and the kinds of uncertainty those works have addressed. Chapter 4 covers the theoretical background of the mathematical methods applied. Chapter 5 goes through the mathematical implementation, detailing how we formulated and implemented the optimization problem. In the last two chapters, we present our results, including plots to illustrate our findings, and then analyze the results and draw conclusions based on the two different mathematical implementations. We finish by explaining what kind of future work is interesting to look at.

2

Home Energy Management System Overview

In this chapter, we provide a general overview of the Home Energy Management System (HEMS) and its role in coordinating household energy use. The following sections describe the system models, key components such as the solar panels, batteries, and household demand, as well as the system's operational rules and requirements. This serves as a foundation for the mathematical formulation introduced in later chapters.

2.1 Details of the HEMS

This section provides a detailed overview of the system configuration and input data used to model the HEMS considered in this work. A HEMS is designed to monitor, control, and optimize a home's energy flows, such as electricity generation from solar panels, storage in batteries, and consumption by household devices and electric vehicles, to reduce costs and improve energy efficiency. In the implementation of our optimization model for the HEMS, we include several system-specific details and input data that are used as assumptions. These elements are not calculated or analyzed in depth but rather serve as fixed inputs to allow us to focus on the core objective of the project.

The modeled household is based on a typical Swedish single-family home with an annual electricity consumption of approximately 20,000 kWh [2], exhibiting seasonal variation primarily driven by temperature. Weather-related data, including ambient temperature and solar irradiance, are obtained from SMHI [13], while electricity spot price data are taken from Nord Pool [11] in the SE3 price region. All historical data cover the period from 2023 to 2024 and are used to model both household demand and solar panel production.

The system includes a BEV with the size 100 kWh capable of charging and discharging at a maximum power of ± 11 kW. Secondly, a RESS is considered in three configurations with storage capacities of 20, 50, and 100 kWh, and corresponding charge/discharge power limits of ± 10, ± 15, and ± 20 kW. Solar energy is integrated through a solar panel system comprising 20 panels, each with an area of 2 m^2, yielding a total installed capacity of 8 kW. The household is also connected to the grid with symmetric import and export limits of ± 11 kW. Additionally, a smart electricity meter is assumed to be in place to facilitate real-time monitoring and control of both energy consumption and production. To provide a clearer overview, all system details and data assumptions are summarized in Table 2.1:

Table 2.1: Summary of HEMS system specifications and input data

Component	Details
Historical Data	SMHI temperature and solar irradiance (2023–2024) Nordpool SE3 spot prices (2023–2024)
Residential Home	Annual demand: 20,000 kWh/year
Solar Panels	20 panels, 2 m^2 each Total installed capacity: 8 kW
RESS	Sizes: 20 / 50 / 100 kWh Max power: ±10 / ±15 / ±20 kW
BEV	Size: 100 kWh Max power: ±11 kW
Grid Connection	Max import/export power: ±11 kW
Energy Meter	Real-time monitoring of consumption and production

2.2 System Model

In this section, we present the system models that form the foundation for the optimization framework. These models describe the key components of the HEMS, including the Solar Panel Model, which provides the power generated from the solar panels; the House Model, which captures the household's electricity consumption; the Battery Model, which manages the behavior of the Battery Electric Vehicle (BEV) and Residential Energy Storage System (RESS) batteries; and the Energy Meter Model, which ensures power balance between the home and the grid.

2.2.1 Solar Panel Model

The electricity generated by the solar panels is represented below. Here P_{solar} denotes the amount of power generated, such that $P_{solar} \geq 0$:

$$P_{solar}(t) = \min\{\eta_{sol} \cdot a_{sol} \cdot I_{sun}(t) \cdot \gamma_{cf}, N_{sol} \cdot P_{sol}^{n}\},$$

where

- η_{sol}: Mean panel conversion efficiency, $\eta_{sol} \in [0, 1]$
- a_{sol}: Surface area of the solar panel, $a_{sol} \in \mathbb{R}$
- $I_{sun}(t)$: Solar irradiance in W/m^2
- γ_{cf}: Capacity factor, $\gamma_{cf} = 1$
- N_{sol}: Number of solar panels, $N_{sol} \in \mathbb{N}$

- P^n_{sol}: Rated power for each panel, $P^n_{sol} \in \mathbb{R}$.

The capacity factor γ_{cf} accounts for the effects of panel orientation, tilt, and shading by scaling of the incoming solar irradiance. In this model, we simplify the formulation by setting $\gamma_{cf} = 1$, assuming ideal conditions.

To illustrate how the solar panel model behaves in practice, Figure 2.1 shows an example of the solar power production ($P_{solar}(t)$) over 24 hours based on historical irradiance data.

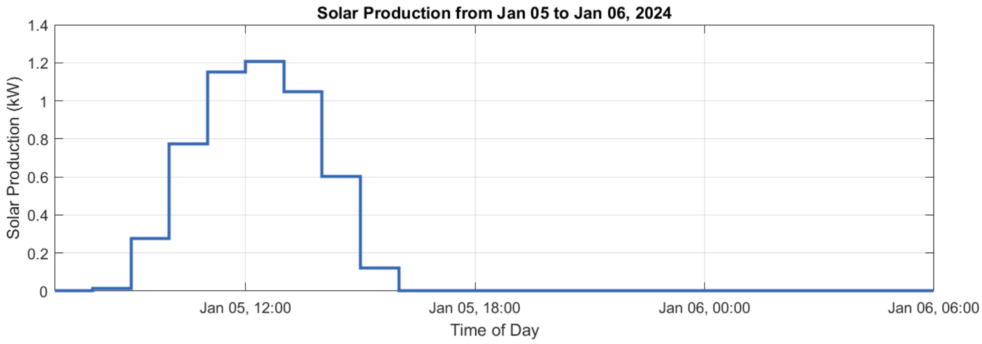

Figure 2.1: Example of the solar production ($P_{solar}(t)$) over 24 hours, starting 07:00 January 5th 2024.

2.2.2 House Model

The power consumed by the house, $P_{home} \leq 0$, depending on the ambient temperature, T_{amb}, and time, t, is described by

$$P_{home}(t) = P_{base}(t) + P_{heat}(T_{amb}(t)) + P_{cool}(T_{amb}(t)),$$

where

- $P_{base}(t)$: Amount of power for the base loads in the house like lights, electronics, kitchen appliances etc. $P_{base} \in \mathbb{R}$
- $P_{heat}(T_{amb}(t))$: Amount of power for the heating of the house and water. $P_{heat}(T_{amb}(t)) \in \mathbb{R}$
- $P_{cool}(T_{amb}(t))$: Amount of power for the cooling of the house. $P_{heat}(T_{amb}(t)) \in \mathbb{R}$

To illustrate how the house model model behaves in practice, Figure 2.2 shows an example of the power consumed by the house ($P_{home}(t)$) over 24 hours based on historical temperature data.

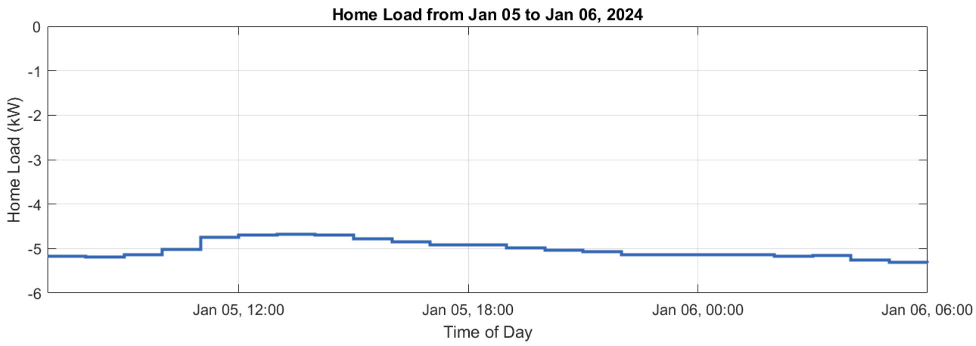

Figure 2.2: Example of the Home Load ($P_{home}(t)$) over 24 hours, starting 07:00 January 5th 2024.

2.2.3 RESS Model

The RESS operates continuously throughout the optimization horizon and is available at all times. Its state is updated using the ordinary differential equation (ODE):

$$\frac{d}{dt}SOE_R = -\frac{1}{E_R} \cdot P \cdot \eta_R \quad \text{s.t. } \eta_R = \begin{cases} \eta_0, & \text{for} \quad P \geq 0 \\ \frac{1}{\eta_0}, & \text{for} \quad P < 0 \end{cases}$$

where:

- SOE_R: SOE of the RESS, $SOE_R \in [0, 1]$
- E_R: Maximum capacity of the RESS, $E_R \in \mathbb{R}$
- P: Battery power (discharge or charge), $P \in \mathbb{R}$
- $\eta_0 \in (0, 1]$: Battery efficiency.

R represents the RESS battery in the set $\mathcal{B} = [B, R]$. Here B represents the BEV battery.

Additionally, the RESS has a fixed initial and target SOE defined by $Target^R_{SOE} \in [0, 1]$. This means that the RESS battery always begins the optimization with $Target^R_{SOE}$ and must ensure that it is recharged to the same level by the end of the horizon.

2.2.4 BEV Model

Unlike the RESS, the BEV is only connected to the system during specific hours, defined by plug-in and plug-out times. Its energy state is thus modeled as:

$$\frac{d}{dt}SOE_B = \begin{cases} -\frac{1}{E_B} \cdot P \cdot \eta_B, & t \in [t_{in}, t_{out}] \\ 0 & \text{otherwise} \end{cases} \quad \text{s.t. } \eta_b = \begin{cases} \eta_0, & \text{for} \quad P \geq 0 \\ \frac{1}{\eta_0}, & \text{for} \quad P < 0 \end{cases},$$

where:

- SOE_B: SOE of the BEV, $SOE_B \in [0, 1]$

- E_B: Maximum capacity of the BEV, $E_B \in \mathbb{R}$
- P: Battery power (discharge or charge), $P \in \mathbb{R}$
- $\eta_0 \in (0, 1]$: Battery efficiency.

The BEV operates similarly to the RESS but has additional constraints due to its plug-in and plug-out times. The plug-in time t_{in} represents when the vehicle returns home and becomes available, and a plug-out time t_{out}, fixed at 07:00, indicates when the vehicle departs and is no longer available for energy exchange. The BEV can only charge or discharge during the time window $t_{in} < t < t_{out}$.

The BEV also has initial and target SOE for the optimization horizon. The initial SOE, denoted $Initial^B_{SOE}$, is the energy level of the BEV at the time of plug-in, t_{in}. The target SOE, denoted $Target^B_{SOE}$, defines the required energy level at the end of the optimization horizon, at t_{out}. The optimization model must thus ensure that the BEV reaches the target SOE by t_{out}.

In this context, it is possible to treat a RESS and a BEV in a similar manner, i.e., as a form of battery, meaning that the same modeling assumptions can be used for both devices. For the remainder of this report, we will adopt this approach, where the BEV is modeled similarly to the RESS with the exception of the fact that the BEV operates in active and non-active stages due to its plug-in and plug-out times. Other than this distinction, the BEV will follow the same functional principles as the RESS.

2.2.5 Energy Meter Model

The energy meter acts as a connection point between a home and the local electrical grid. The power balance equation at the energy meter is given by the equation

$$P_{home}(t) + P_{solar}(t) = P_{sell}(t) - P_{buy}(t) - \sum_{b \in \mathcal{B}} (P_{d,b}(t) - P_{c,b}(t)),$$

where

- $P_{buy}(t)$: Amount of power bought at time t. $P_{buy}(t) \geq 0$
- $P_{sell}(t)$: Amount of power sold at time t. $P_{sell}(t) \geq 0$
- $P_{d,b}(t)$: Discharging power of battery $b \in \mathcal{B}$ at time t. $P_{d,b}(t) \geq 0$
- $P_{c,b}(t)$: Charging power of battery $b \in \mathcal{B}$ at time t. $P_{c,b}(t) \geq 0$

2.2.6 Electricity Price Model

In this report, we consider two main models for electricity pricing: a spot-price model and a Demand-Charge Tariff (DCT) model.

1. **Spot-Price Model:**
   In the spot-price model, the electricity price varies hourly according to the market spot price. The total cost of electricity consumption is determined by the energy consumed each hour, multiplied by the corresponding spot price.

Additionally, it is possible to sell electricity back to the grid; however, the price received for selling is lower than the price paid for purchasing, due to taxes and other associated fees. The spot prices for buying and selling electricity for the 5th of January can be seen in Figure 2.3.

2. **Demand-Charge Tariff Model**
   The DCT model builds upon the spot-price model by adding a penalty based on the daily peak power demand, which is captured by the DCT. In this model, the cost of electricity consumption includes both the energy purchased at the hourly spot price and the penalty associated with the peak demand during the optimization horizon. The DCT penalty is calculated daily based on the highest power demand within a 24-hour period, with a simplified approach that does not account for the timing within the month. As with the spot-price model, the cost of purchasing electricity is higher than the income when selling it back to the grid.

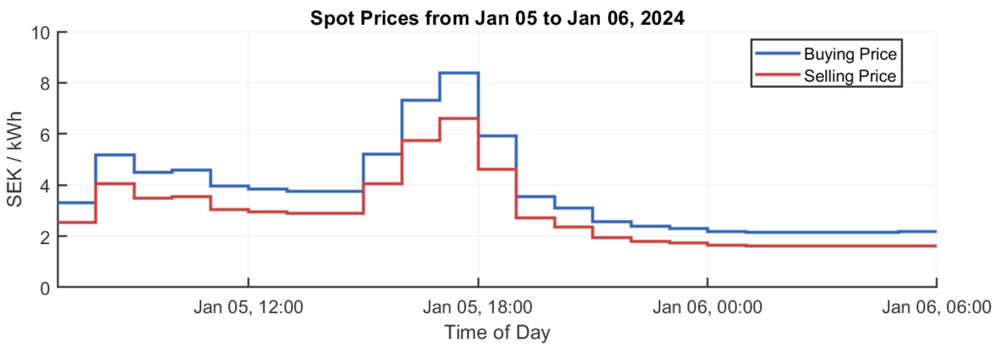

Figure 2.3: Example of spot prices for buying and selling electricity over 24 hours, starting 07:00 January 5th 2024.

3
Previous Work

Optimizing energy use in smart homes has been widely studied, especially in systems that combine renewable energy, storage, and electric vehicles. This section highlights relevant research that has shaped current approaches to HEMS optimization, focusing on different methods, assumptions, and objectives that relate to our work. Before we examine what research has been done in this subject, we first provide a brief overview of the purpose of HEMS optimization and the types of mathematical methods that can be used.

3.1 HEMS Optimization

A HEMS helps a household manage its energy use in a smart and efficient way. It can, for example, decide when to charge a home battery or an electric vehicle, based on energy availability and cost. The system typically includes the home itself, solar panels, a RESS, and a BEV.

The main idea behind HEMS optimization is to use energy as efficiently and cost effective as possible. To achieve this, different optimization methods can be used to plan and control how energy is consumed and stored. The goal is to find the best way to operate everything in the household based on the available information. These optimization methods generally fall into two categories: mathematical techniques and heuristic techniques.

3.1.1 Mathematical Techniques

- Linear Programming
- Mixed Integer Linear Programming

Mathematical modeling is used to simulate a system when the system is not overly complex and can be described using known physical laws. In such cases, relationships between systems parameters are derived analytically based on prior knowledge of the system's behavior. This approach is particularly effective when the nature on non-linearity is well understood, allowing for simplifications or assumptions that make the model more manageable and interpretable. However, mathematical modeling becomes challenging for highly complex systems, as deriving exact solutions may require intricate equations and extensive computational resources. Additionally, achieving an accurate representation often require to make trade-offs between model fidelity/accuracy and computational feasibility [9].

3.1.2 Heuristic Techniques

- Particle Swarm Optimization
- Genetic Algorithm
- Gray Wolf Algorithm

Heuristic (or meta-heuristic) techniques are designed to solve complex optimization and decision-making problems by implementing natural phenomena. Unlike mathematical modeling, these techniques do not require prior knowledge of the system's underlying equations or non-linearity structure, making them suitable for problems where relationships between parameters are unknown or too complex to derive analytically. This makes them great and efficient in solving high-dimensional, non-linear, and multi-objective problems without the need for simplifying assumptions. They can also improve precision and accuracy by refining solutions iteratively making them well-suited for optimization where dynamic and uncertain conditions are prevalent. However, they are in this case often computationally intensive, require large amounts of data, and may not always guarantee a globally optimal solution [9].

3.2 Mixed Integer, known BEV arrival time

In the realm of mixed-integer formulations with known BEV schedules, two key studies stand out. [5] use a single-stage mixed-integer linear program (MILP) over a 24-hour, 15-minute time grid to co-optimize household loads, a residential battery and an electric vehicle under perfect foresight. Their price-threshold charging strategy, and explicit limits on battery cycling, delivers up to 31 % in combined cost savings, while CPLEX finds the exact optimum in seconds versus minutes for heuristic solvers. Building on this, [4] splits the problem into a two-stage MILP: first minimizing daily energy costs, then using the same assets for reactive-power support to improve local power factor. By linearizing nonlinear constraints, their approach retains computational efficiency and demonstrates that cost reductions and power-quality gains can be achieved simultaneously. Together, these works highlight MILP's power under ideal forecasts and point to the value of extending such models to handle uncertainty.

3.3 Stochastic Programming

In the stochastic programming domain, [6] replace fixed EV schedules with a dynamic model that captures real-world driving uncertainty. They frame BEV charging as a stochastic dynamic program, using an inhomogeneous Markov chain to represent the likelihood of departures, returns and trip lengths throughout the day. By balancing the goal of low charging costs against a penalty for leaving the vehicle undercharged, their rolling-horizon approach continuously adapts decisions based on current state-of-charge, expected trips and fluctuating electricity prices. Tested on 2½ months of training data and 2 months of out-of-sample validation, this method cuts daily charging costs by 19–47% compared to simple rule-of-thumb strategies.

3.4 Mixed Integer, Stochastic driving schedule

[14] use a MILP model that injects uncertainty directly into the optimization by generating scenarios for EV arrival and departure, photovoltaic (PV) output, initial battery state-of-energy and dynamic electricity prices. With bidirectional trading enabled, the model applies prioritization rules to decide when to sell energy back to the grid under V2G operation. Tested across Monte Carlo–derived scenarios, this stochastic MILP consistently cuts expected system costs versus a comparable deterministic schedule. Although they curb unnecessary EV cycling through constraints, detailed battery degradation modeling is left for future work.

3.5 Meta-Heuristic Optimization Methods

Meta-heuristic algorithms like Binary Particle Swarm Optimization (BPSO) offer a flexible way to tackle the complex, multi-objective nature of HEMS optimization. [10] frame the problem as balancing cost minimization, peak-load shaving and user satisfaction, arguing that traditional LP, MILP or dynamic programming methods struggle with high dimensionality and convergence. Their BPSO implementation efficiently handles the on/off scheduling of numerous appliances, achieving a 52.47% reduction in electricity costs and an additional 29.41% savings by selling surplus energy back to the grid. Building on this approach, [7] apply BPSO to real-time–pricing demand response in a smart home equipped with PV generation, battery storage and an electric vehicle. By coordinating electrical and thermal loads according to tariff signals, renewable availability, and user comfort preferences, they deliver significant cost savings while reducing peak grid draw by 9.636 kW, demonstrating that BPSO can simultaneously address affordability, resilience, and comfort.

3.6 Electricity Price Models, with Demand Charge Tariffs, without BEV

Demand-Charge Tariffs (DCT), which bill customers based on their highest peak consumption within a billing cycle, add a new layer of complexity to Home Energy Management Systems. One clear illustration is provided by [8], who develop a mixed-integer, nonlinear HEMS model that tackles both real-time pricing (RTP) costs and monthly DCT penalties in one framework. They point out that simply shifting loads to off-peak periods can unintentionally raise your monthly peak and your DCT bill, so they introduce a "day-index" weighting coefficient that makes the scheduler increasingly sensitive to peak demand as the month advances. Because the resulting problem is high-dimensional and nonlinear, [8] turn to a meta-heuristic

Natural Aggregation Algorithm rather than a conventional solver. In a one-month simulation, their approach not only lowers daily energy costs but also noticeably trims monthly peak-demand charges, demonstrating the value of horizon-aware load scheduling.

3.7 Previous Work Summary

After reviewing these and other studies, we found no examples of a linear optimization method that directly incorporates uncertainty. This absence suggests either that the approach has not yet been explored or published, or that it may face practical limitations. Regardless, it makes the idea worth investigating.

What makes this line of work especially interesting is the efficiency of linear models. While they may not always provide the highest accuracy, they are computationally effective and highly scalable. This makes them well-suited for applications involving many parallel systems, such as large groups of homes or electric vehicles, where computational demand quickly becomes a bottleneck. By keeping the formulation linear, we ensure the model remains scalable and adaptable, making it suitable for both small-scale setups and larger setups involving multiple different scenarios.

4
Theory

In this chapter, we provide a theoretical background on the various areas relevant to our problem implementation.

4.1 Linear programming

A Linear Programming (LP) problem is an optimization problem where both the objective function and constraints are linear. The goal is to determine the optimal values of decision variables that either minimize or maximize a given linear function while satisfying a set of linear constraints.

The standard formulation of an LP problem is:

$$\begin{aligned} \min_{x} \quad & c^T x \\ \text{subject to} \quad & Ax = b, \end{aligned} \tag{4.1}$$

where

- x – Decision variable vector.
- c – Coefficient vector of the objective function.
- A – Matrix representing the coefficients of the constraints.
- b – Right-hand side vector of the constraints.

4.2 Stochastic programming

A Stochastic Programming (SP) problem is a mathematical optimization framework used to model decision-making problems involving uncertainty. Unlike deterministic optimization, where all inputs and parameters are known and fixed, stochastic programming accounts for uncertain elements. The goal of a SP problem is to find a solution that not only optimizes a chosen objective but also performs well across a range of possible future scenarios.

4.2.1 Two-stage Stochastic Programming

The basic idea of two-stage SP is that decisions should be made based solely on the information available at the time of decision making, without relying on knowledge of future outcomes. The general two-stage SP problem can be formulated as in [12]

$$\min_{x \in X} \left\{ g(x) := c^T x + \mathbb{E}[Q(x, \xi)] \right\}, \tag{4.2}$$

where $Q(x, \xi)$ is the optimal value of the second-stage problem

$$\min_{y} q^T y \quad \text{subject to} \quad Tx + Wy \leq h. \tag{4.3}$$

This means that in a two-stage SP problem, we make a first-stage "here-and-now" [12] decision $x \in \mathbb{R}^n$, before the uncertainty $\xi = (q, T, W, h)$ is realized. After the realization of ξ, a second-stage decision $y \in \mathbb{R}^m$ is made by solving a corresponding optimization problem that adapts to the revealed outcome. The goal thus become to minimize the first-stage cost, $c^T x$, plus the expected (optimal) second-stage cost [12].

The general two-stage problem described above is classified as a linear program, as both its objective functions and constraints are linear. It can be further reformulated as follows:

$$\begin{aligned} \min_{x \in \mathbb{R}^n} \quad & g(x) = c^T x + \mathbb{E}[Q(x, \xi)] \\ \text{s.t.} \quad & Ax = b \\ & x \geq 0 \end{aligned} \tag{4.4}$$

where $Q(x, \xi)$ is defined as

$$\begin{aligned} \min_{y \in \mathbb{R}^m} \quad & q(\xi)^T y \\ \text{s.t.} \quad & T(\xi)x + W(\xi)y = h(\xi) \\ & y \geq 0. \end{aligned} \tag{4.5}$$

4.2.2 Scenario-based approach

When we formulated the two-stage SP problem in section 4.2.1, a key assumption is that the second-stage data ξ can be modeled as a random vector with a known probability distribution. This assumptions holds in many practical cases, particularly when the distribution of ξ can be reliably estimated from historical data and is relatively stable over time. However, in many real-world scenarios, such precise probabilistic information is unavailable. Moreover, for numerical solution methods, it is often necessary to approximate the uncertainty by assuming that ξ can take a finite number of possible realizations, called *scenarios*. In this case, the random vector is represented as $\xi \in \{\xi_1, ..., \xi_k\}$ where each scenario ξ_K occurs with an associated probability $p_k > 0$, for $p_1, ..., p_K$, such that $\sum_{k=1}^{K} p_k = 1$ [12].

Considering this scenario split, the expectation in the first-stage problem's objective function (4.2) can be written as:

$$\mathbb{E}[Q(x, \xi)] = \sum_{k=1}^{K} p_k Q(x, \xi_k).[12] \tag{4.6}$$

With this formulation of the expected value, the two-stage problem can be reformulated as a large linear programming problem (see 5.1.2).

The scenario approach effectively unfolds the stochastic problem into a tree structure, where each branch represents possible realization of the uncertain parameters and their corresponding decisions (see Figure 4.1).

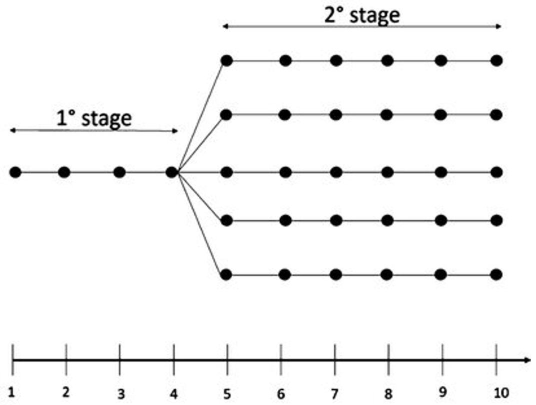

Figure 4.1: Two-stage SP problem represented by a scenario tree [1].

Scenarios are typically constructed from historical data or generated using statistical models that reflect the expected variation in uncertain inputs. The quality of these scenarios, how well they represent the true underlying uncertainty, has a direct impact on the quality of the resulting solution.

4.2.3 Deterministic equivalent stochastic programming

To enable numerical solution and retain a structured representation of uncertainty, the two-stage stochastic linear problem can be reformulated into its deterministic equivalent. This is done by approximating the uncertainty in the second-stage data through a finite set of scenarios, each associated with a probability. In this formulation, the expected value term in the objective function is replaced by a weighted sum over all scenarios. This transformation preserves the essence of the stochastic problem while enabling the use of conventional optimization techniques, such as linear programming, to obtain solutions that account for multiple possible realizations of uncertainty.

The standard form of deterministic equivalent problem to a stochastic problem is:

$$
\begin{aligned}
\min_{x,\,y,\,z_k} \quad & f^T x + g^T y + \sum_{k=1}^{K} p_k h_k^T z_k \\
\text{s.t.} \quad & Tx + Uy = r, \\
& V_k y + W_k z_k = s_k, \quad k = 1, 2, \ldots, K \\
& x, y, z_1, z_2, \ldots, z_K \geq 0,
\end{aligned}
\tag{4.7}
$$

where the decision variables are:

- x, y – First-stage decision variables, determined before uncertainty is realized.
- z_k – Second-stage decision variables for scenario k, which adjust after uncertainty is revealed.

and the coefficients and parameters are:

- f, g – Cost coefficients for the first-stage decision variables.
- h_k – Cost coefficients for the second-stage decision variable z_k in scenario k.
- p_k – Probability of scenario k, used to weight the expected cost in the objective function.
- T, U – Matrices defining constraints in the first stage.
- V_k, W_k – Matrices defining constraints in the second stage, specific to each scenario k.
- r, s_k – Right-hand side parameters defining constraints in the first and second stages.

4.3 Demand-Charge Tariffs

As energy systems become increasingly decentralized and flexible, the structure of electricity pricing plays a crucial role in shaping consumer behavior. Traditional models such as Time-of-Use and Real-Time Pricing (RTP) encourage users to shift energy consumption from expensive peak periods to cheaper off-peak hours. While effective in reducing energy bills, these approaches primarily target energy usage (kWh) rather than addressing peak power demand (kW), which is a critical factor in grid stability and infrastructure sizing.

To more directly influence peak loads, Demand-Charge Tariffs (DCTs) have been introduced. These schemes charge users not only for total energy consumed, but also for their maximum power draw over a billing period. DCTs have long been standard for industrial and commercial customers, where managing peak demand is financially significant. However, with the growing presence of energy-intensive technologies in residential homes, such as BEVs, RESSs, and rooftop solar panels, there is an increasing momentum to extend such pricing models to households as well. Research and pilot programs have shown that DCTs can encourage load smoothing and reduce the peak-to-valley ratio of household demand [8]. While these findings are well-established, their practical relevance has only grown.

In fact, the importance of DCTs is now being reflected in regulatory action. In Sweden, nationwide implementation of DCTs for residential customers is underway and will be fully rolled out by 1 January 2027. Several regions have already begun transitioning, and this shift underscores the need for energy systems, particularly optimization models, to account for peak-sensitive pricing. However, the specific design of these tariffs varies significantly depending on the local power grid company, which is responsible for delivering electricity to households in a given area [3].

A common method is to calculate the demand charge based on the average of the three highest power peaks (in kW) within a monthly billing period, applying a fixed cost per kW to discourage short-term spikes. Some operators use flat rates throughout the day, while others apply time-differentiated charges, penalizing peak power use more heavily during daytime hours and less so at night. This dual-rate model encourages not only reduced consumption but smarter timing.

Despite these differences, the goal is the same: to lower peak demand and ease pressure on local grids. For optimization models and home energy systems, incorporating these tariff structures is essential for accurately reflecting real-world costs and behaviors.

5

Implementation

5.1 Mathematical Implementation

In the section we will introduce the mathematical implementations of the HEMS optimization problem. We will begin by defining a linear problem formulation in section 5.1.1 and then define the problem as a deterministic equivalent stochastic problem (DESP) in section 5.1.2. Finally, we will also introduce a DESP implementation that takes demand-based tariffs into consideration in section 5.2.

5.1.1 Linear Problem Formulation

The proposed Home Energy Management System (HEMS) is firstly modeled using linear programming to achieve cost minimization over a 24-hour time horizon. The scheduling focuses on the Battery Electric Vehicle (BEV) and Renewable Energy Storage System (RESS). The cost function of the proposed HEMS includes the costs associated with purchasing and selling electricity to the grid. By optimizing the scheduling of the BEV and RESS, we aim to minimize the overall energy costs for the home.

5.1.1.1 Linearization of the Battery Models

Due to the non-linear behavior of the efficiency parameter η_b, which depends on the sign of the power component P, we reformulate the two battery models (sections 2.2.3 and 2.2.4) to achieve linearity. As explained in those sections, both the BEV and RESS are modeled in a similar manner, allowing us to treat them in the same way. Linearization is performed by splitting P into two separate variables. A discharge component $P_d \geq 0$ and a charge component $P_c \geq 0$. This transformation eliminates the sign dependency and simplifies the optimization process to:

$$\frac{d}{dt}SOE_b(t) = -\frac{1}{E_b}\left(P_d(t) \cdot (1+\delta) - P_c(t) \cdot (1-\delta)\right), \tag{5.1}$$

where:

- δ: Loss during energy conversion. $\delta \in [0, 1]$
- $P_d(t)$: Battery discharge power. $P_d(t) \geq 0$
- $P_c(t)$: Battery charge power. $P_c(t) \geq 0$

- $SOE_b(t)$: State of Energy for battery b at time t, $SOE \in [0, 1]$

and b represents a specific battery within the set $\mathcal{B} = [B, R]$. Where B and R represent the BEV and RESS battery respectively.

To implement the battery constraint in our numerical linear model, we discretize it over time. Assuming a fixed time step of $\Delta t = 1$. This time resolution matches the structure of our optimization problem, which operates on an hourly basis and receives updated inputs such as electricity prices every hour.

$$\frac{d}{dt}SOE_b(t) \approx SOE_b(t+1) - SOE_b(t) \tag{5.2}$$

$$\Rightarrow \quad SOE_b(t+1) = SOE_b(t) - \frac{1}{E_b}\left(P_d(t) \cdot (1+\delta) - P_c \cdot (t)(1-\delta)\right) \tag{5.3}$$

Expanding the expression gives:

$$SOE_b(t+1) = SOE_b(t) + \frac{1}{E_b}(1-\delta) \cdot P_c(t) - \frac{1}{E_b}(1+\delta) \cdot P_d(t) \tag{5.4}$$

This is the recursive update of the differential equation (5.1).

5.1.1.2 Decision variables

To optimize HEMS and minimize electricity costs, we consider a set of decision variables that influence the household's energy operation. These variables represent the free variables in our mathematical model and determine how the system allocates energy consumption, storage, and interaction with the grid at each time step. Specifically, each decision variable is modeled as a vector with one entry per time step in the optimization horizon, resulting in a time-indexed set of decisions that collectively guide the behavior of the system throughout the period.

Electricity Transactions with the Grid
The amount of electricity purchased from the grid (P_{buy}) and the amount sold back to the grid (P_{sell}) must be determined dynamically. These decisions depend on factors such as electricity prices, energy demand, and available storage capacity.

Battery Charging and Discharging Behavior
To efficiently utilize energy storage, we need to decide how much energy each battery should charge and discharge at any given moment. The RESS has two key decision variables the charging power (P_{cR}) and the discharging power (P_{dR}). Similarly the BEV has (P_{cB}) and (P_{dB}).

State of Energy of the Batteries
At each time step, we also need to monitor the state of charge of both the BEV and RESS (SOE_B, SOE_R). The SOE decision variable helps us ensure that there is enough power stored for future use while preventing overcharging.

5.1.1.3 Cost

Our goal is to minimize electricity costs for homeowners but there are a few important factors to consider when it comes to pricing. The cost of buying electricity is higher than the price received when selling it back to the grid ($c_{buy}(t) > c_{sell}(t)$). This is because purchased electricity includes the spot price plus taxes and other fees, while selling electricity back to the grid provides a lower return than the price one would pay to buy electricity at the same moment.

5.1.1.4 Objective function and LP problem

The objective function to the LP problem is given by:

$$J = \sum_{t=1}^{24} \sum_{i=1}^{8} \mathcal{C}_{t,i} \mathcal{Z}_{i,t} = \sum_{t=1}^{24} \mathbf{c}_t^T \mathbf{z}_t = \mathbb{c}^T \mathbb{z}, \tag{5.5}$$

The cost matrix $\mathcal{C} \in \mathbb{R}^{24\times 8}$ accounts for the varying electricity prices throughout the day:

$$\mathcal{C} = \begin{bmatrix} c_{buy}(1) & c_{sell}(1) & 0 & \dots & 0 \\ c_{buy}(2) & c_{sell}(2) & 0 & \dots & 0 \\ \vdots & \vdots & 0 & \ddots & \vdots \\ c_{buy}(24) & c_{sell}(24) & 0 & \dots & 0 \end{bmatrix}. \tag{5.6}$$

Similarly, the decision variable matrix $\mathcal{Z} \in \mathbb{R}^{8\times 24}$ is defined as:

$$\mathcal{Z} = \begin{bmatrix} P_{buy}(1) & P_{buy}(2) & \dots & P_{buy}(24) \\ P_{sell}(1) & P_{sell}(2) & \dots & P_{sell}(24) \\ P_{cR}(1) & P_{cR}(2) & \dots & P_{cR}(24) \\ P_{dR}(1) & P_{dR}(2) & \dots & P_{dR}(24) \\ SOE_R(1) & SOE_R(2) & \dots & SOE_R(24) \\ P_{cB}(1) & P_{cB}(2) & \dots & P_{cB}(24) \\ P_{dB}(1) & P_{dB}(2) & \dots & P_{dB}(24) \\ SOE_B(1) & SOE_B(2) & \dots & SOE_B(24) \end{bmatrix}. \tag{5.7}$$

Each vector $\mathbf{c}_t$ corresponds to a row of the matrix $\mathcal{C}$ and represents the cost of buying or selling power to the grid at a specific time step t. Likewise, each $\mathbf{z}_t$ corresponds to a column of the matrix $\mathcal{Z}$ and represents the decision variables at that time step.

To make the objective function and the LP problem more adaptable to our implementation, we define it as:

$$\underset{\mathbb{z}}{\text{minimize}} \quad \mathbb{c}^T \mathbb{z} \tag{5.8a}$$

$$\text{subject to} \quad A\mathbb{z} = b. \tag{5.8b}$$

Here $A \in \mathbb{R}^{m \times n}$ is the constraint matrix, and $b \in \mathbb{R}^m$ is the right-hand side vector containing the constants of the equality constraints. The new vector $\mathbb{c} \in \mathbb{R}^{192}$ is derived from its corresponding matrix $\mathcal{C}$ by stacking its columns in column-major order. This transformation creates a single long vector from the matrix, making it easier to work with in the optimization process. If we let $\mathcal{C}(t,i)$ denote the element in the t-th row and i-th column of the matrix $\mathcal{C}$, the corresponding position in the vector $\mathbb{c}$ is given by:

$$\mathbb{c}(k) = \mathcal{C}(t,i), \tag{5.9}$$

where the index k is determined as:

$$k = t + 24 \cdot (i-1), \quad \text{for } 1 \leq t \leq 24, \quad 1 \leq i \leq 8. \tag{5.10}$$

Similarly to the cost vector $\mathbb{c}$, the new vector $\mathbb{z} \in \mathbb{R}^{192}$ is also reshaped from its corresponding matrix $\mathcal{Z}$. However, unlike $\mathbb{c}$, it will be formed in row-major order. If we let $\mathcal{Z}(i,t)$ denote the element in the i-th row and t-th column, the corresponding position in the vector $\mathbb{z}$ is given by:

$$\mathbb{z}(k) = \mathcal{Z}(i,t), \tag{5.11}$$

where the index k is determined as in (5.10).
The reason for this reformulation of the problem in (5.8) is to simplify the optimization process and align the problem with the standard input structure required by linear programming solvers. This allows us to efficiently use tools like the `linprog` function in MATLAB, which is designed for vectorized formulations.

Using the provided data and incorporating all relevant constraints, we explicitly construct the constraint matrix A, thereby fully formulating the optimization model (5.8). The size and structure of A, as well as its individual components, are determined by the constraints defined in equation (5.12).

$$\min_{\mathbb{z}} \quad \mathbb{c}^T \cdot \mathbb{z}$$

Subject to

$$P_{solar}(t) = \min\{\eta_{sol} \cdot A_{sol} \cdot I_{sun}(t) \cdot \gamma_{cf}, N_{sol} \cdot P_{sol}^{n}\} \tag{5.12a}$$

$$P_{home}(t) = P_{base}(t) + P_{heat}(T_{amb}(t)) + P_{cool}(T_{amb}(t)) \tag{5.12b}$$

$$SOE_B(t+1) = SOE_B(t) + \frac{1}{E_B}(1-\delta) \cdot P_{cB}(t) - \frac{1}{E_B}(1+\delta) \cdot P_{dB}(t) \tag{5.12c}$$

$$SOE_R(t+1) = SOE_R(t) + \frac{1}{E_R}(1-\delta) \cdot P_{cR}(t) - \frac{1}{E_R}(1+\delta) \cdot P_{dR}(t) \tag{5.12d}$$

$$P_{home}(t) + P_{solar}(t) = P_{sell}(t) - P_{buy}(t) - \sum_{b \in \mathcal{B}} (P_{d,b}(t) - P_{c,b}(t)) \tag{5.12e}$$

$$SOE_B(1) = SOE_B(24) = Target_{SOE}^{B} \tag{5.12f}$$

$$SOE_R(1) = SOE_R(24) = Target_{SOE}^{R} \tag{5.12g}$$

$$P_{solar}, P_{buy}, P_{sell} \geq 0 \quad \forall t \tag{5.12h}$$

$$P_{home} \leq 0 \quad \forall t \tag{5.12i}$$

$$P_{cR}^{min} = P_{dR}^{min} = -10, -15, -20 \quad \forall t \tag{5.12j}$$

$$P_{cR}^{max} = P_{dR}^{max} = 10, 15, 20 \quad \forall t \tag{5.12k}$$

$$P_{cB}^{min} = P_{dB}^{min} = -11 \quad \forall t \tag{5.12l}$$

$$P_{cB}^{max} = P_{dB}^{max} = 11 \quad \forall t \tag{5.12m}$$

$$SOE_R^{min} = SOE_B^{min} = 0 \quad \forall t \tag{5.12n}$$

$$SOE_R^{max} = SOE_B^{max} = 1 \quad \forall t \tag{5.12o}$$

$$\tag{5.12p}$$

In this formulation, there is no uncertainty. All parameters are assumed to be known and deterministic. This allows the optimization problem to be solved efficiently as a linear program using MATLAB's `linprog` function.

5.1.2 Deterministic Equivalent Stochastic Problem

Although the linear program provides an initial evaluation of costs, it does not account for the uncertainties inherent in the system. To address this, we transform the problem into a deterministic equivalent stochastic problem (DESP) that can still be solved as a linear program.

This scenario-based formulation supports an arbitrary number of possible future outcomes. Each scenario represents a distinct realization of uncertain parameters, such as electricity prices, solar production, or the SOE upon arrival of the BEV. The optimization then seeks decisions that are robust across all scenarios, weighted by their associated probabilities.

In the main body of this report, we focus on the case where the uncertainty lies in the arrival SOE of the BEV. To simplify the analysis and enhance interpretability, we consider two representative scenarios: one extreme (e.g., low arrival SOE) and one nominal (close to expected values). Additionally, we include in Appendix A.1.1 an alternative formulation where the electricity price is treated as the uncertain variable. In this case, the system configuration excludes the BEV, allowing us to isolate the impact of price volatility on the optimization.

While we present only one source of uncertainty at a time for clarity, the proposed method can naturally accommodate multiple uncertain variables simultaneously, making it well-suited for more comprehensive real-world applications.

5.1.2.1 Uncertainty in arrival State of Energy

In this section we focus on the uncertainty associated with the arrival SOE for the BEV. We consider two distinct scenarios: one where the BEV arrives with a high SOE, and another where it arrives with a low SOE. Each scenario is assigned a probability $p_s \in [0, 1]$ with $\sum p_s = 1$, reflecting the likelihood of each scenario in the set $\mathcal{S}$. Additionally, we define u_1 as the number of first-stage decision variables per time step, and u_2 as the number of second-stage (scenario-dependent) decision variables per time step. To maintain generality, we now denote the number of time steps as $\mathcal{T}$, rather than fixing it to 24 as done previously. This allows the formulation to accommodate arbitrary time resolutions.

From Equation (4.7), we then derive the objective function as:

$$\mathcal{J} = \mathbb{c}^T \mathbb{x} + \sum_{s \in \mathcal{S}} p_s \mathbb{c}_s^T \mathbb{y}_s, \tag{5.13}$$

where:

- $\mathbb{c} \in \mathbb{R}^{u_1 \mathcal{T}}$ and $\mathbb{c}_s \in \mathbb{R}^{u_2 \mathcal{T}}$ are cost vector for the first-stage and second-stage (scenario dependent) decisions, respectively,
- $\mathbb{x} \in \mathbb{R}^{u_1 \cdot \mathcal{T}}$ is the first-stage decision vector,
- and $\mathbb{y}_s \in \mathbb{R}^{u_2 \cdot \mathcal{T}}$ is the second-stage decision vector for scenario s.

The first-stage decision vector is stacked by variable across all time steps:

$$\mathbb{x} = \begin{bmatrix} \mathbf{P}_{buy} \\ \mathbf{P}_{sell} \\ \mathbf{P}_{cR} \\ \mathbf{P}_{dR} \\ \mathbf{SOE}_R \end{bmatrix} = \begin{bmatrix} P_{buy}(1) \\ \vdots \\ P_{buy}(t_{in}) \\ P_{sell}(1) \\ \vdots \\ SOE_R(t_{in}) \end{bmatrix}. \tag{5.14}$$

Similarly, for each scenario $s \in \mathcal{S}$, the second-stage decision vector is given by

$$\mathbb{y}_s = \begin{bmatrix} \mathbf{P}^s_{buy} \\ \mathbf{P}^s_{sell} \\ \mathbf{P}^s_{cR} \\ \mathbf{P}^s_{dR} \\ \mathbf{SOE}^s_R \\ \mathbf{P}^s_{cB} \\ \mathbf{P}^s_{dB} \\ \mathbf{SOE}^s_B \end{bmatrix} = \begin{bmatrix} P^s_{buy}(t_{in}) \\ \vdots \\ P^s_{buy}(\mathcal{T}) \\ P^s_{sell}(t_{in}) \\ \vdots \\ SOE^s_B(\mathcal{T}) \end{bmatrix}. \tag{5.15}$$

To simplify notation, we introduce t_{in} as the last hour from the first stage in the DESP. This implies that the the first stage range from $[1, t_{in}]$.

The constraints remain mostly unchanged from (5.12). However, for each scenario, we introduce an additional set of specific constraints that are influenced by the uncertainty.

For the number of scenarios in $\mathcal{S}$ ($|\mathcal{S}|$) we get the following constraints:

Constraints that do not change depending on scenarios:

$$P_{solar}(t) = \min\{\eta_{sol} \cdot A_{sol} \cdot I_{sun}(t) \cdot \gamma_{cf}, N_{sol} \cdot P^n_{sol}\}, \quad \forall t \tag{5.16a}$$
$$P_{home}(t) = P_{base}(t) + P_{heat}(T_{amb}(t)) + P_{cool}(T_{amb}(t)), \quad \forall t \tag{5.16b}$$
$$P_{home}(t) + P_{solar}(t) = P_{sell}(t) - P_{buy}(t) - P_{dR}(t) + P_{cR}(t), \quad t \in [1, t_{in}] \tag{5.16c}$$
$$SOE_R(t+1) = SOE_R(t) + \frac{1}{E_R}(1-\delta) \cdot P_{cR} - \frac{1}{E_R}(1+\delta) \cdot P_{dR}, \quad t \in [1, t_{in}] \tag{5.16d}$$
$$SOE_B(1) = SOE_B(\mathcal{T}) = Target^B_{SOE} \tag{5.16e}$$
$$SOE_R(1) = SOE_R(\mathcal{T}) = Target^R_{SOE} \tag{5.16f}$$
$$P_{solar}, P_{buy}, P_{sell} \geq 0 \quad \forall t \tag{5.16g}$$
$$P_{home} \leq 0 \quad \forall t \tag{5.16h}$$
$$P^{min}_{cR} = P^{min}_{dR} = -10, -15, -20 \quad \forall t \tag{5.16i}$$
$$P^{max}_{cR} = P^{max}_{dR} = 10, 15, 20 \quad \forall t \tag{5.16j}$$
$$P^{min}_{cB} = P^{min}_{dB} = -11 \quad \forall t \tag{5.16k}$$
$$P^{max}_{cB} = P^{max}_{dB} = 11 \quad \forall t \tag{5.16l}$$
$$SOE^{min}_R = SOE^{min}_B = 0 \quad \forall t \tag{5.16m}$$
$$SOE^{max}_R = SOE^{max}_B = 1 \quad \forall t \tag{5.16n}$$
$$\tag{5.16o}$$

Constraints that vary based on the number of scenarios s, where $s = 1, .., |\mathcal{S}|$ for time steps $t \in [t_{in}, \mathcal{T}]$:

$$P^s_{home}(t) + P^s_{solar}(t) = P^s_{sell}(t) - P^s_{buy}(t) - \sum_{b\in\mathcal{B}} \left(P^s_{d,b}(t) - P^s_{c,b}(t)\right) \tag{5.17a}$$

$$SOE^s_R(t+1) = SOE^s_R(t) + \frac{1}{E_R}(1-\delta)\cdot P^s_{cR} - \frac{1}{E_R}(1+\delta)\cdot P^s_{dR} \tag{5.17b}$$

$$SOE^s_B(t+1) = SOE^s_B(t) + \frac{1}{E_B}(1-\delta)\cdot P^s_{cB} - \frac{1}{E_B}(1+\delta)\cdot P^s_{dB}. \tag{5.17c}$$

Additionally, we introduce new constraints to manage the transition between stages and to prevent selling or buying during inactive stages.

Stage transition constraints:

$$SOE_R(t_{in}) - SOE^s_R(t_{in}) = 0 \quad \forall s \tag{5.18a}$$

$$P_{sell}(t) = \begin{cases} 0 \text{ for } t \in [t_{in}+1, \mathcal{T}] \\ \text{otherwise (5.16c)} \end{cases} \tag{5.18b}$$

$$P_{buy}(t) = \begin{cases} 0 \text{ for } t \in [t_{in}+1, \mathcal{T}] \\ \text{otherwise (5.16c)} \end{cases} \tag{5.18c}$$

$$P^s_{sell}(t) = \begin{cases} 0 \text{ for } s = 1, \dots, |\mathcal{S}|, \quad t \in [1, t_{in}] \\ \text{otherwise (5.17a)} \end{cases} \tag{5.18d}$$

$$P^s_{buy}(t) = \begin{cases} 0 \text{ for } s = 1, \dots, |\mathcal{S}|, \quad t \in [1, t_{in}] \\ \text{otherwise (5.17a).} \end{cases} \tag{5.18e}$$

5.1.2.2 Illustrative Example: Two Scenarios

For visualization purposes, we present the formulation for the specific case of two scenarios related to the uncertainty in the BEV's arrival SOE. This simplified example illustrates how the scenario-based structure of the model is applied when considering a limited number of possible outcomes.

$$P_{solar} = \min\{\eta_{sol} \cdot A_{sol} \cdot I_{sun}(t) \cdot \gamma_{cf}, N_{sol} \cdot P_{sol}^{n}\} \tag{5.19a}$$
$$P_{home} = P_{base}(t) + P_{heat}(T_{amd}(t)) + P_{cool}(T_{amb}(t)) \tag{5.19b}$$
$$P_{home}(t) + P_{solar}(t) = P_{sell}(t) - P_{buy}(t) - P_{dR}(t) + P_{cR}(t) \tag{5.19c}$$
$$P_{home}^{1}(t) + P_{solar}^{1}(t) = P_{sell}^{1}(t) - P_{buy}^{1}(t) - \sum_{b \in \mathcal{B}} \left(P_{d,b}^{1}(t) - P_{c,b}^{1}(t)\right) \tag{5.19d}$$
$$P_{home}^{2}(t) + P_{solar}^{2}(t) = P_{sell}^{2}(t) - P_{buy}^{2}(t) - \sum_{b \in \mathcal{B}} \left(P_{d,b}^{2}(t) - P_{c,b}^{2}(t)\right) \tag{5.19e}$$
$$SOE_R(t+1) = SOE_R(t) + \frac{1}{E_R}(1-\delta) \cdot P_{cR} - \frac{1}{E_R}(1+\delta) \cdot P_{dR} \tag{5.19f}$$
$$SOE_R^1(t+1) = SOE_R^1(t) + \frac{1}{E_R}(1-\delta) \cdot P_{cR}^1 - \frac{1}{E_R}(1+\delta) \cdot P_{dR}^1 \tag{5.19g}$$
$$SOE_R^2(t+1) = SOE_R^2(t) + \frac{1}{E_R}(1-\delta) \cdot P_{cR}^2 - \frac{1}{E_R}(1+\delta) \cdot P_{dR}^2 \tag{5.19h}$$
$$SOE_B^1(t+1) = SOE_B^1(t) + \frac{1}{E_B}(1-\delta) \cdot P_{cB}^1 - \frac{1}{E_B}(1+\delta) \cdot P_{dB}^1 \tag{5.19i}$$
$$SOE_B^2(t+1) = SOE_B^2(t) + \frac{1}{E_B}(1-\delta) \cdot P_{cB}^2 - \frac{1}{E_B}(1+\delta) \cdot P_{dB}^2 \tag{5.19j}$$
$$SOE_R(t_{in}) - SOE_R^1(t_{in}) = 0 \tag{5.19k}$$
$$SOE_R(t_{in}) - SOE_{R(}^2 t_{in}) = 0 \tag{5.19l}$$
$$P_{sell}(t) = \begin{cases} 0 \text{ for } t \in [t_{in}+1, \mathcal{T}] \\ \text{otherwise (5.19c)} \end{cases} \tag{5.19m}$$
$$P_{buy}(t) = \begin{cases} 0 \text{ for } t \in [t_{in}+1, \mathcal{T}] \\ \text{otherwise (5.19c)} \end{cases} \tag{5.19n}$$
$$P_{sell}^{s}(t) = \begin{cases} 0 \text{ for } s = 1, 2, \quad t \in [1, t_{in}] \\ \text{otherwise (5.19d) / (5.19e)} \end{cases} \tag{5.19o}$$
$$P_{buy}^{s}(t) = \begin{cases} 0 \text{ for } s = 1, 2, \quad t \in [1, t_{in}] \\ \text{otherwise (5.19d) / (5.19e).} \end{cases} \tag{5.19p}$$
$$SOE_B(1) = SOE_B(\mathcal{T}) = Target_{SOE}^{B} \tag{5.19q}$$
$$SOE_R(1) = SOE_R(\mathcal{T}) = Target_{SOE}^{R} \tag{5.19r}$$
$$P_{solar}, P_{buy}, P_{sell} \geq 0 \quad \forall t \tag{5.19s}$$
$$P_{home} \leq 0 \quad \forall t \tag{5.19t}$$
$$P_{cR}^{min} = P_{dR}^{min} = -10, -15, -20 \quad \forall t \tag{5.19u}$$
$$P_{cR}^{max} = P_{dR}^{max} = 10, 15, 20 \quad \forall t \tag{5.19v}$$
$$P_{cB}^{min} = P_{dB}^{min} = -11 \quad \forall t \tag{5.19w}$$
$$P_{cB}^{max} = P_{dB}^{max} = 11 \quad \forall t \tag{5.19x}$$
$$SOE_R^{min} = SOE_B^{min} = 0 \quad \forall t \tag{5.19y}$$
$$SOE_R^{max} = SOE_B^{max} = 1 \quad \forall t \tag{5.19z}$$

Compared to the original formulation in Equation (5.12), it is clear that the problem size and thereby complexity increase significantly when incorporating uncertainty. Even with only two scenarios, the size of the optimization problem grows substantially. This increase in dimensionality underscores how quickly the problem scales with additional scenarios. In the next section, we quantify this growth by examining how the size of the constraint matrix evolves with varying numbers of scenarios.

5.1.2.3 Memory storage of different scenarios

Most of our calculations will be performed with two scenarios. The reason for this is that, in our case, we are only calculating for a single car, whereas in the real world, this would be done for many different cars, significantly increasing the computational complexity. This also means that as the size of A increases, the computation time will also grow. Furthermore, if multiple sources of uncertainty, such as both BEV arrival SOE and electricity prices, are considered simultaneously, the problem size and memory requirements would grow even more rapidly due to the combinatorial increase in the number of scenarios. To illustrate how much A expands depending on the number of scenarios, we have created Table 5.1.

Table 5.1: Memory storage depending on size of matrix A

Nr. Scenarios (s)	**Dimension of** A (**dim**(A))	**Memory storage (kB)**
1 scenarios	194×72	55
2 scenarios	509×96	191
3 scenarios	703×120	330
4 scenarios	897×144	505
$\vdots$	$\vdots$	$\vdots$
10 scenarios	2061×288	2 320
$\vdots$	$\vdots$	$\vdots$
s scenarios	$(121 + 194 \cdot s) \times (48 + 24 \cdot s)$	$(N_A \cdot 4)/1024$

Here N_A is the number of elements in the matrix A.

5.2 Demand-Charge Tariffs

To reflect the increasing prevalence of Demand-Charge Tariffs (DCTs), which at the moment are being introduced in Sweden and will be mandatory by 2027, we incorporate a simplified version of such pricing structures in our model. Traditionally, these tariffs impose a monthly charge based on the customer's highest, or a set of highest, power peaks within the billing period. Often with varying rates depending on the time of day or season. However, to reduce computational complexity and improve model tractability, we implement a simplified approach where the daily maximum power demand is identified and penalized accordingly given a constant flat rate throughout the day. This method preserves the core incentive of demand-charge pricing, reducing peak loads, while allowing for easier integration into the HEMS optimization framework.

To introduce the demand-based tariffs, we modify the objective function as follows:

$$\mathcal{J} = c^T \mathbf{x}_t + \sum_{s \in \mathcal{S}} p_s c_s^T \mathbf{y}_{t,s} + \omega \cdot \sum_{s \in \mathcal{S}} p_s \|P_{buy}^s\|_\infty. \tag{5.20}$$

Here, the additional term involving the infinity norm of the bought grid power, P_{buy}, scaled by a tariff penalty coefficient ω, serves to penalize high power peaks. By including $\|P_{buy}\|_\infty$, we effectively capture the maximum power drawn from the grid during the optimization horizon, which aligns with the structure of DCTs. This encourages the HEMS to shift or reduce loads to minimize peak demand.

Additionally, we add the following constraints to linearize (5.20):

$$P_{buy}^s(t) - P_{peak}^s \leq 0 \tag{5.21a}$$

$$-P_{buy}^s(t) - P_{peak}^s \leq 0 \tag{5.21b}$$

Where the auxiliary variable P_{peak}^s represents the maximum power imported from the grid in scenario s, and is used to model the infinity norm $\|P_{buy}^s\|_\infty$ in a linear form. The two constraints ensure that for all time steps t, the grid import $P_{buy}^s(t)$ remains bounded by P_{peak}^s in both the positive and negative directions. As a result, P_{peak}^s effectively captures the largest absolute value of grid power import over the horizon in scenario s.
This formulation allows us to include the peak demand cost in the objective function while keeping the optimization problem linear:

$$\mathcal{J} = c^T \mathbf{x}_t + \sum_{s \in \mathcal{S}} p_s c_s^T \mathbf{y}_{t,s} + \omega \cdot \sum_{s \in \mathcal{S}} p_s P_{peak}^s. \tag{5.22}$$

5.3 Algorithm

In order to describe our workflow and how we approach solving the problem in MATLAB, we introduce an algorithm in this section that sequentially incorporate both deterministic and stochastic methods. We first implemented the deterministic LP model over a full 24-hour horizon, assembling a single constraints matrix and defining all decision-variable bounds in order to compute and plot the BEV/RESS trajectories and calculate the total cost. Building on this, we extended the code to a two-scenario stochastic optimization: we created a larger matrix with additional constraints and solved the resulting Deterministic Equivalent Stochastic Problem, again over a 24-hour horizon, but now accounting for two possible arrival SOE scenarios when the car comes home. After this, we conducted a case study where we included a realization of the car's actual arrival SOE. Once the BEV arrives and its actual SOE is known, we switch back to the original LP model, using the realized data to optimize charging and discharging for the remaining hours until departure. This realization step is key, as it allows us to fairly compare the stochastic solution with the deterministic one, using the same real outcome in both cases.

Algorithm 1

Step 1: LP

Assemble constraint matrix **A**, set bounds and solve optimization over 24 h using LP.

Store cost and trajectories for BEV/RESS

Step 2: Introduce two-scenario uncertainty

Expand matrix **A** to include the scenario based constraints and solve over 24h

Store cost and trajectories for BEV/RESS

Step 3: Realization of new information

Car arrives and the actual arrival SOE is realized and stored.

Step 4: Re-optimize remaining time

Switch back to the deterministic LP and re-optimize for remaining hours before departure.

Step 5: Compare Solutions

Compare LP and Stochastic optimization during winter and summer.

To compare solutions we look over a longer time period and find out how extreme days effect the optimization.

Although the algorithm above is our main focus, we have also developed a variant that incorporates Demand-Charge Tariffs (DCT) into the optimization, but this version excludes the realization phase.

Algorithm 2 : Optimization with DCT

Step 1: Include DCT

Apply the same algorithm as above to the 24-hour horizon, but use an alternative price model for the optimization.

Store cost and trajectories for BEV/RESS

Store amount of power bought from the grid

Step 2: Compare trajectories and power from grid

Compare optimization with and without DCT, compare trajectories and the power bought from grid for LP and DESP.

Step 3: Compare solutions over longer time period

Compare DESP with DCT built into the optimization versus applied only after optimization, evaluated over an extended time horizon.

5.4 Assumptions in the Implementation

We have made several assumptions in our study. In this section, we will review each assumption and explain the reasoning behind them. Some of these assumptions are based on Volvo's recommendations and previous study, while others have been made to simplify the problem.

5.4.1 Home

In our assumptions, we consider all relevant details about the household such as size, the presence of solar panels, and other key factors to be known. This means that our analysis is tailored to a specific type of house, and the results may not be directly applicable to all households but it can be changed to different characteristics and varying energy consumption patterns. We assume that these variations would not cause a major change in the overall results.

5.4.1.1 Household energy demand

We assume that the household's electricity demand at each time step, given the ambient temperature, is known in advance. However, in real-world applications, this assumption may not hold, as household consumption patterns can vary unpredictably. For instance, a resident might not always use the oven at the same time each day or could unexpectedly operate several appliances simultaneously, resulting in fluctuations in energy demand. While such variations could affect the optimization outcomes, we deliberately exclude this to limit the scope. However, such uncertainties can also be modelled using scenarios.

5.4.2 Batteries (BEV and RESS)

We do not take into consideration any degradation of the BEV battery. However, this would be a crucial factor in a more detailed analysis, as battery aging over time affects both performance and long-term efficiency. While discharging the battery to save 20 SEK in a single day might seem beneficial, it could ultimately result in a greater loss, due to the reduced lifespan and value of the battery. However with the information and time available, it is difficult to determine exactly the cost associated with potential battery degradation.

5.4.2.1 SOE and time of arrival

We do not know the car's SOE until it arrives home, but in a real-time scenario, this would not be the case. Through an app you could monitor the car's status and send a signal in advance when it is on its way home. Also as a user you could estimate your arrival time and input it manually.

5.4.3 Electricity prices

We use historical data for our implementation, but it can easily be adjusted to reflect real-time prices. In Sweden, electricity prices for the upcoming day are published the day before, around noon. According to [11], the prices for the next day become available at 14:15. At that time, you can see the electricity prices for the next 33.75 hours, whereas at 14:00, only the next 10 hours are visible. However, our goal

is not to track electricity prices in real time but rather to compare uncertainty in parameters overall, using all known data. This uncertainty can also be modelled through scenarios, which we have presented in Appendix A.1.1.
We assume that the household we have is billed under an hourly spot-prices, but it is important to note that alternative pricing models exist. For example a housing cooperative (bostadsrättsförening) may instead negotiate a fixed electricity price for all apartments, resulting in a different cost structure.

5.4.4 Weather

We use historical weather data for our implementation, but it can easily be adjusted to reflect real-time forecasts. In Sweden weather forecasts are updated regularly throughout the day, with detailed predictions available up to 10 days in advance and hourly updates for the next 48 hours. In our implementation we also assume we know in advance exactly how much solar power each solar panel produce depending on the weather, as we are not currently focusing on the uncertainty associated with the solar panels or weather. However, weather is usually unreliable and therefore this could be a factor worth exploring in the future, which can also be examined using scenarios.

5.5 Non feasible solutions

In some situations, especially when the BEV arrives late with a very low SOE, it may not be possible to fully meet all system constraints. Such as reaching a high target SOE within a limited time frame. These cases represent instances of infeasibility, which are inherent to constrained optimization problems involving variable inputs and physical limitations.

While all scenarios presented in this work are feasible by design, a general system might benefit from more advanced methods for handling such cases. For instance, one could formulate the charging target as a required amount of energy rather than a fixes SOE level. Alternatively, soft constraints or adaptive relaxation of targets could be used to ensure that the optimization always returns a solution, even when exact goals cannot be met.

However, for this work, our main focus was on modeling, scenario formulation, and analyzing the impacts of uncertainty. Implementing a more advanced handling of infeasibility was outside the scope and timeline of the project.

6

Results and Discussion

This chapter presents the key findings from the optimization of the Home Energy Management System (HEMS), with a focus on the impact of uncertainty in the Battery Electric Vehicle's (BEV) arrival State of Energy (SOE). The analysis is based on a stochastic programming approach, formulated as a Deterministic Equivalent Stochastic Problem (DESP), allowing us to evaluate how uncertainty in BEV behavior influences system operation and overall electricity cost.

While the DESP formulation is general and adaptable to multiple sources of uncertainty and any number of scenarios, this study concentrates on a single source of uncertainty, the BEV's arrival SOE, and primarily explores two representative scenarios to facilitate interpretation and visualization. These scenarios serve to highlight how variation in vehicle usage patterns can affect the optimal operation of both the BEV and the Residential Energy Storage System (RESS).

To evaluate the benefit of incorporating uncertainty, the stochastic approach is compared directly to a deterministic linear optimization method that assumes perfect foresight of all system parameters. We compare the two methods in two stages. First, over the full 24-hour horizon, we analyze how each method schedules the charging and discharging of both the BEV and the RESS. Second, we introduce a two-stage evaluation process that better reflects real-world conditions: before the BEV arrives, the stochastic model plans for multiple possible arrival SOEs. Once the BEV actually arrives and its true SOE is realized, we re-optimize the remaining hours using this observed value, treating it as a known input. This allows us to assess how each method performs under real-world conditions and to quantify the potential advantages of planning under uncertainty.

Throughout the results, we systematically explore how different system configurations and external conditions influence the optimization framework by:

- **Comparing different electricity price conditions**, including winter days with more volatile electricity prices and summer days with more stable prices.
- **Evaluating different battery system configurations**, including:
  - A **Typical Current Battery System**, with a 20 kWh storage capacity and 10 kW charging/discharging power, representing systems available on the market today (2025).
  - Two **potential future battery systems**:
    * **Future Battery System A**, with a capacity of 50 kWh and a charg-

ing / discharging power of 15 kW.

  * **Future Battery System B**, with a capacity of 100 kWh and a charging / discharge power of 20 kW.

- **Varying operational conditions**, such as the initial SOE of the BEV and its arrival time, to analyze their impact on optimal charging.

Each of these aspects are examined at different stages of the results to understand their influence on system performance and cost savings.

6.1 Baseline Linear Programming Implementation

To build a strong foundation for our work and gain a deeper understanding of the HEMS optimization process, we implemented our own LP model defined in Section 5.1.1, assuming perfect knowledge of all parameters and no uncertainties. While similar implementations already has been developed, creating our own version allowed us to fully grasp the structure of the optimization problem and ensured that the subsequent methods we develop are based on a well-understood framework. Moreover, this also serves as a baseline for comparison between the results in the following sections.

To demonstrate the functionality of the LP implementation Figure 6.1 show the optimized charging trajectories of both the BEV and the RESS for one day. In this case, the BEV arrives at 16:00 with an initial SOE of 50%. As shown in the plot, both the BEV and RESS are discharged during the peak hours to minimize energy costs. Subsequently, both systems charge back to their target SOEs during the night, when spot prices are generally lower.

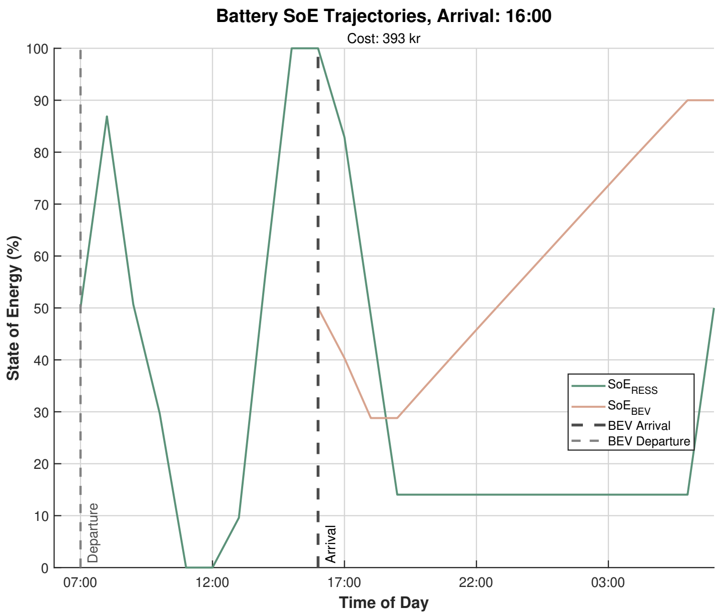

Figure 6.1: Optimized charging trajectories of the BEV and RESS for a single day, with the BEV arriving at 16:00 with 50% SoE and leaving at 7.00 with target SoE of 90%.

6.2 Cost Sensitivity to BEV Arrival Time in a LP Setting (w/o Tariffs)

To analyze how sensitive the total cost of the LP problem is to the BEV arrival time under different seasonal conditions, Figure 6.2 illustrates the cost variations over a single day for both a winter day with high spot price volatility and a summer day with more stable electricity prices. These results are obtained for a **typical current battery system**.

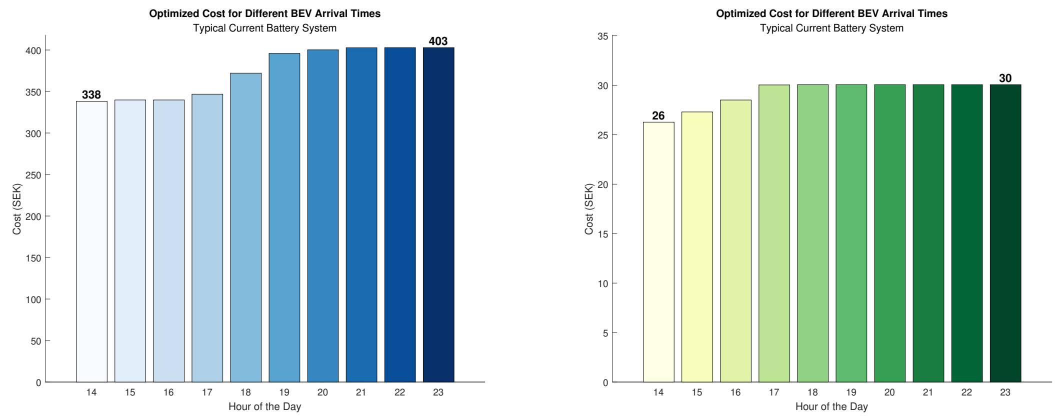

(a) Winter day **(b)** Summer day

Figure 6.2: Cost differences for various BEV arrival times on one winter (5 Jan 2024) and one summer day (1 Jul 2024) for a typical current battery system. Initial SOE 50%, target SOE 90%.

In the plot on the left, we see the energy cost for a winter day with an average outdoor temperature of –15°C, where the car arrives home with 50% state of energy. The bars show how the cost varies depending on the time of arrival. On the right, we see a similar analysis for a summer day, again with the car arriving with 50%, but at different times.
For the winter day, cost fluctuations remain minimal before and after the peak load period. However, a significant cost increase occurs when the BEV arrives during peak load hours, typically between 16:00 and 19:00. Outside of this peak window, the specific arrival time has a negligible impact on overall costs. For example, the cost difference between an arrival at 14:00 versus 15:00, or at 22:00 versus 23:00, is relatively small compared to the largest cost difference (65 SEK).

In contrast, for this specific summer day, the arrival time has an even smaller effect on total costs. The difference in cost across various arrival times is at most 4 SEK, indicating that, under these conditions, BEV arrival time is not a significant factor in cost optimization.

While the structure of cost fluctuations remains similar across the winter and summer day, the total electricity cost on the winter day is substantially higher, about ten times more expensive than on the summer day. This large discrepancy can be attributed to several factors. First, winter days typically exhibit significantly higher household electricity demand due to increased heating needs. In contrast, summer homeloads are generally much lower, especially in Sweden where the use of air conditioning is uncommon. Second, electricity prices tend to be elevated during winter, further amplifying total costs. Third, summer conditions offer much higher solar generation, which not only reduces the reliance on grid electricity but also creates opportunities to sell excess energy back to the grid, offsetting consumption costs. Together, these seasonal differences in demand, pricing, and solar availability explain the contrast in total electricity costs.

However, when analyzing **potential future battery systems**, the sensitivity to BEV arrival time may change. Figures 6.3 and 6.4 present the results for **Future Battery System A** and **Future Battery System B**, respectively.

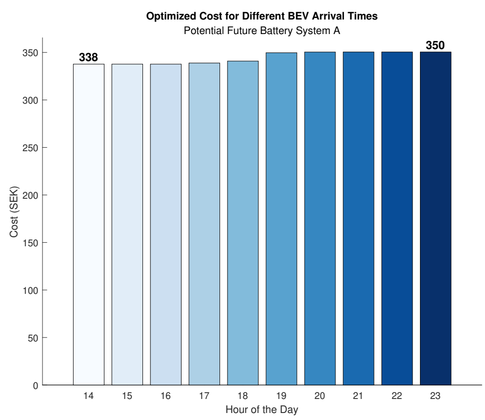

(a) Winter day

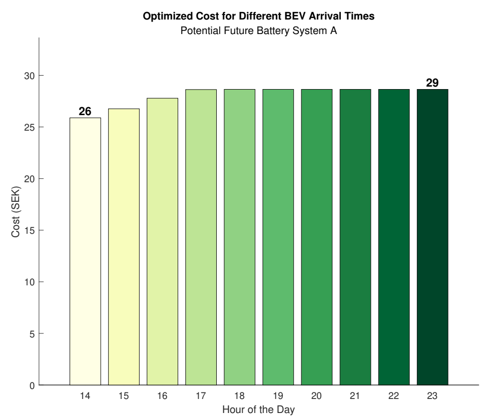

(b) Summer day

Figure 6.3: Cost differences for various BEV arrival times on one winter (5 Jan 2024) and one summer (1 Jul 2024) day for Future Battery System A. Initial SOE 50%, target SOE 90%.

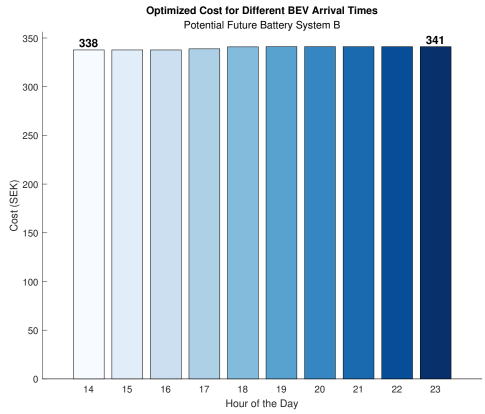

(a) Winter day

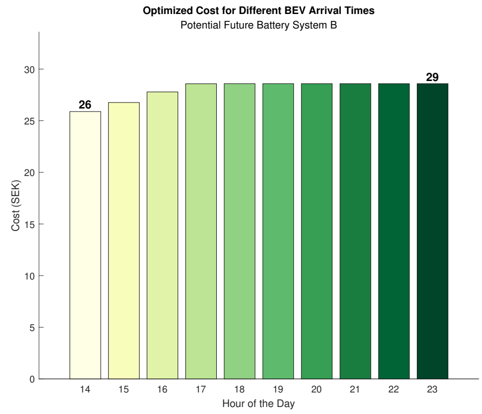

(b) Summer day

Figure 6.4: Cost differences for various BEV arrival times on one winter and one summer day for Future Battery System B. Initial SOE 50%, target SOE 90%.

In these plots, we show the energy cost for the same day using larger battery systems. The top plots correspond to Future Battery System A, while the bottom plots show results for Future Battery System B. As before, the left column represents a winter day and the right column shows a summer day. In all cases, the car arrives with 50% SOE.

The results shown in Figures 6.3 and 6.4 highlight the impact of the BEV arrival time on cost when using larger potential future battery systems. We observe that, as the battery size increases, the sensitivity of the optimization to the arrival time decreases. For example, in the winter day scenario, the cost difference previously observed (65 SEK for the typical current system) is significantly reduced to only 12 SEK for Future Battery System A and 3 SEK for Future Battery System B. This reduction indicates that, for larger battery systems, the timing of the BEV's arrival has a considerably smaller impact on overall costs. For the summer day, the differences are even smaller, as expected, since the cost variation was already minimal for the typical current battery system. This effect is likely due to the increased capacity and charging power, which provide greater flexibility in managing energy use.

To gain a better understanding of how the BEV arrival time affects costs beyond a single day, we now aggregate the results over multiple days in Figure 6.5 and 6.6. For this analysis, we will focus on the two extreme battery system cases: the typical current battery system and Future Battery System B, excluding Future Battery System A for conciseness. Results for Future Battery System A can be found in A.2.1.

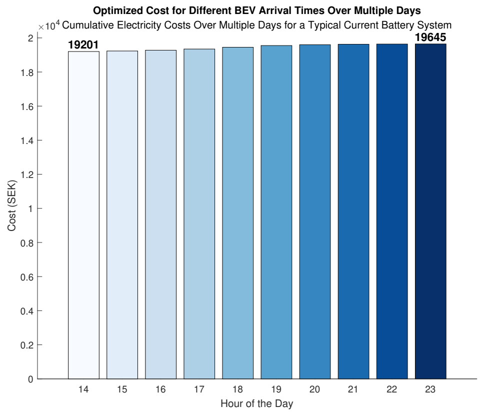

(a) Winter day

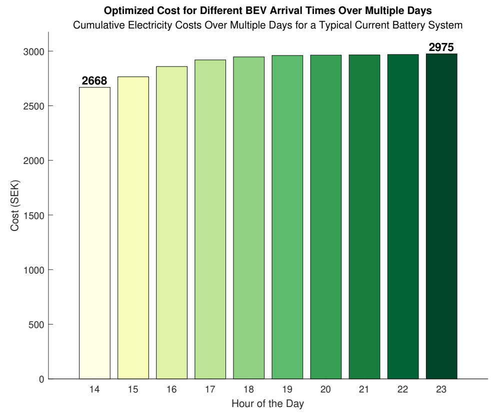

(b) Summer day

Figure 6.5: Cost differences for various BEV arrival times on 100 winter days (fr. 1 Dec 2023) and 100 summer days (fr. May 2024) for a typical current battery system. Initial SOE 50%, target SOE 90% each day.

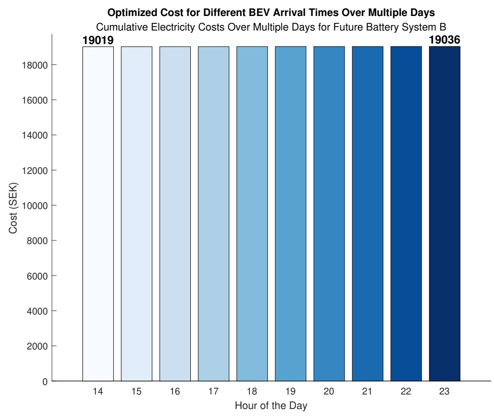

(a) Winter day

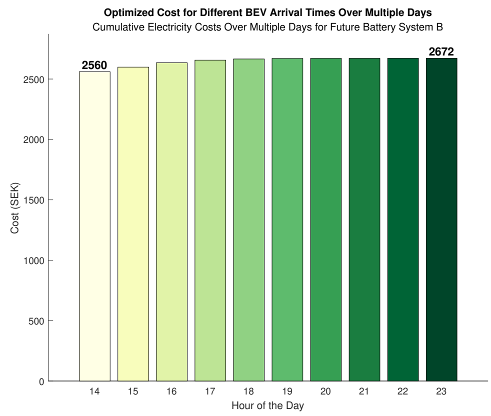

(b) Summer day

Figure 6.6: Cost differences for various BEV arrival times on 100 winter days (fr. 1 Dec 2023) and 100 summer days (fr. 1 May 2024) for Future battery system B. Initial SOE 50%, target SOE 90% each day.

These plots confirm the trend observed in the single-day analysis: cost variations remain most pronounced during peak load hours, especially for the typical current battery system. However, when aggregated over 100 days, the cost differences between arrival times become less distinct, particularly in the winter months. While the general pattern remains, where BEV arrivals during peak hours lead to higher costs, the effect is less extreme over multiple days compared to a single volatile day.

For summer days, the results align closely with the single-day observations, where arrival time has minimal impact on cost. For the winter months however, the larger Future Battery System B further reduces cost differences across different arrival times, reinforcing the trend that larger battery capacities mitigate the sensitivity of cost to arrival time.

Overall, these findings confirm that cost sensitivity to BEV arrival time is highest for smaller batteries and decreases with larger storage capacities. However, when aggregated over multiple days, these effects become less pronounced, indicating that while strategic BEV scheduling, regarding arrival time, remains relevant, it may be less critical over long-term operations for battery systems with larger storage capacities. Given this, we now shift our focus to the main uncertainty: the BEV's SOE upon arrival.

6.3 Uncertainty in BEV Arrival SOE

To extend the optimization framework and account for uncertainty in the BEV's SOE upon arrival, a Deterministic Equivalent Stochastic Problem (DESP) was formulated, as described in Section 5.1.2.

6.3.1 Visualization of DESP Results

In this section, we show how uncertainty influences the results, we first compare the SOE trajectories of the RESS in both stages, for different numbers of scenarios. We then contrast these with the "perfect foresight" solution, obtained by solving a separate linear program for each scenario as if it were known in advance. A bar chart of the associated costs makes the comparison clear. Additionally, we present the BEV SOE trajectories for the scenarios. Once the BEV arrives, the trajectories show how the optimization adjusts its charging and discharging behavior based on the specific scenario.

6.3.1.1 BEV/RESS Trajectories DESP

To illustrate the impact of seasonal price variations, we present optimization results for a specific winter day and a specific summer day. In each case, the BEV arrives at a certain time under two different scenarios, characterized by varying SOE levels upon arrival and associated probabilities. The plots presented are generated on the basis of an optimization performed using a typical current battery system.

Figures 6.7a and 6.7b illustrate the results for the selected winter day. The first figure presents the SOE trajectories of the RESS along with a cost comparison between the stochastic and deterministic solutions, while the second figure displays the corresponding SOE trajectories of the BEV.

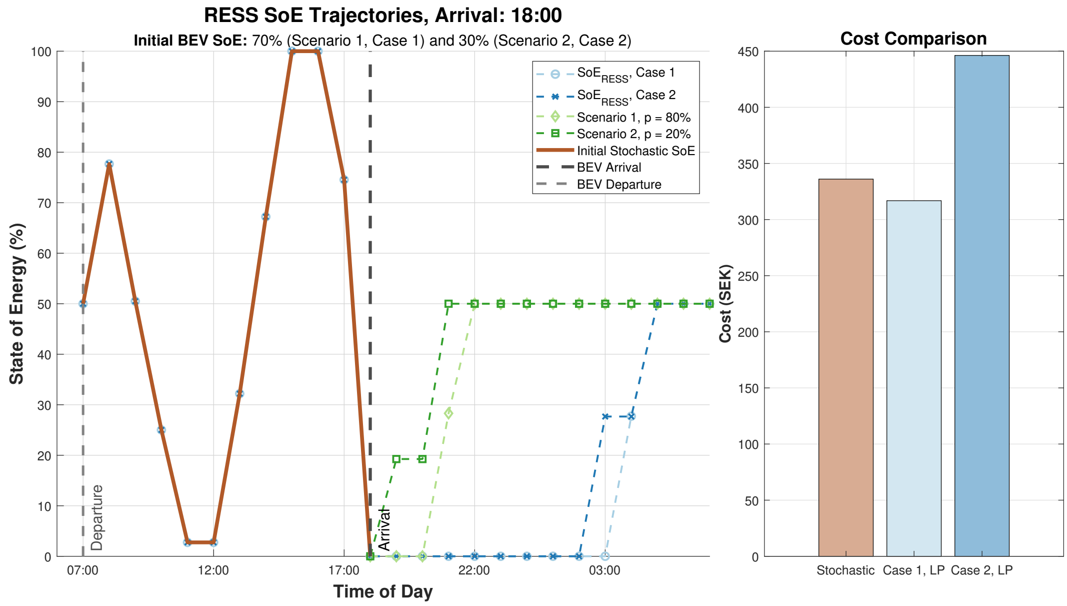

(a) RESS SOE trajectories and cost comparison for a winter day (5 Jan 2024). BEV arrives at 18:00 and leaves at 7:00 with a target SoE of 80%. Scenario 1 assumes a BEV arrival SoE of 70%, while Scenario 2 assumes 30%.

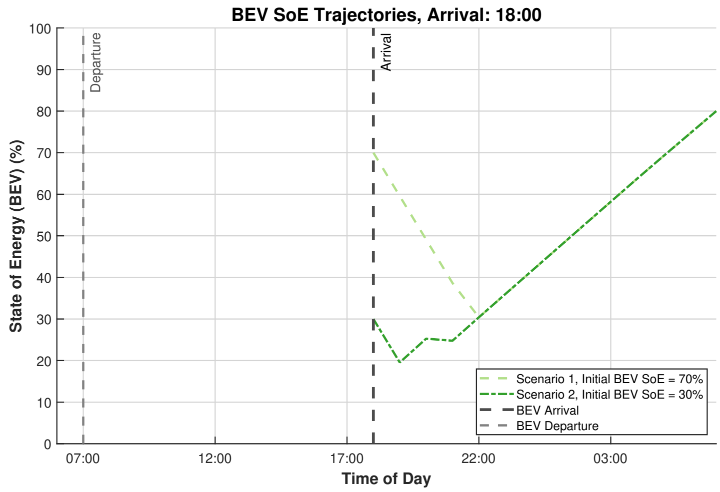

(b) BEV SOE trajectories for the same winter day, with identical arrival/departure schedule and target SoE. Scenario 1: arrival SoE = 70%. Scenario 2: 30%.

Figure 6.7: SOE trajectories of both the RESS and BEV on a winter day (5 Jan 2024) under two BEV arrival SoE scenarios.

6.7a compares LP and stochastic optimization by plotting RESS trajectories and a bar chart of total daily costs. On the left, the RESS charge profile for a winter day (BEV out 07:00–18:00) is shown in red; behind it, the LP and stochastic curves coincide with a 20 kWh battery. After the car returns, the stochastic case splits into two green curves (70 % SOE light, 30 % SOE dark), each recalculated on arrival, while the LP yields two blue curves (also 70 % and 30 % SOE). The stochastic model uses a single pre-arrival trajectory; LP requires one each.

On the right, a cost bar chart shows total household expenses for: the stochastic solution (80 % probable on 70 % arrival SOE, 20 % on 30 %) and the two deterministic cases (known 70 % or 30 % arrival SOE), covering all energy use.

6.7b shows the BEV's charging trajectory from its arrival until departure, but only for the stochastic optimization. The light green curve assumes a 70 % SOE on arrival, while the dark green curve assumes 30 %.

Similarly, Figures 6.8a and 6.8b show the results for the selected summer day, maintaining the same scenario variations but under a different electricity price profile.

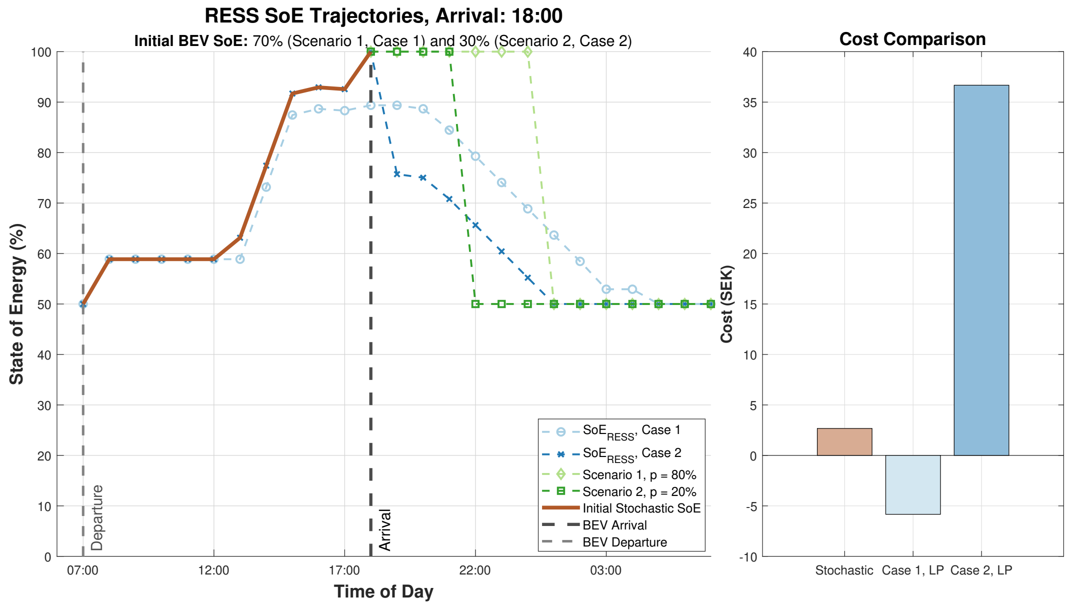

(a) RESS SOE trajectories and cost comparison for a summer day (1 Jul 2024). The BEV arrives at 18:00 and leaves at 7:00 with a target SoE of 80%. Scenario 1 assumes a BEV arrival SoE of 70%, while Scenario 2 assumes 30%.

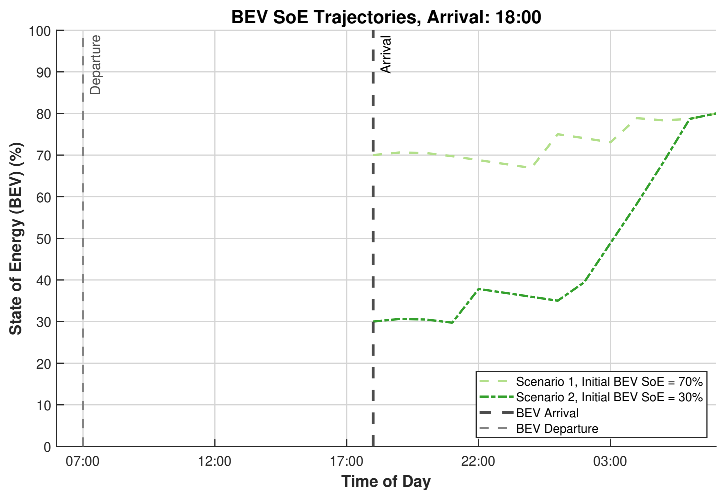

(b) BEV SOE trajectories for the same summer day. The BEV follows the same schedule, but with a target SoE of 80%. Scenario 1 assumes arrival SoE of 70%, Scenario 2 assumes 30%.

Figure 6.8: SOE trajectories of both the RESS and BEV on a summer day (1 Jul 2024) under two BEV arrival SoE scenarios.

In Figure 6.8a, we replicate the trajectories from Figure 6.7a for a summer day (1 Jul 2024), again using a 20 kWh home battery. Note that in the right-hand plot the

LP Case 1 cost is negative—this reflects net revenue, since excess electricity is sold back to the grid.

In Figure 6.8b, we replicate the trajectories from Figure 6.7b for a summer day.

Figures 6.7-6.8 reveal clear trends for both winter and summer days, where the BEV and RESS batteries both charge during periods of low electricity prices and discharge during peak hours. However, this behavior is more pronounced on winter days possibly due to greater price volatility. The RESS trajectories, in particular, are very similar in both the stochastic and deterministic optimization solutions until the BEV arrives, highlighting that the RESS system operates in a predictable manner regardless of the optimization approach for a typical current battery system.

Notably, in one of the deterministic cases during the summer, the RESS battery can actually sell energy for a profit, as indicated by the negative cost in Figure 6.8a.

The cost differences between the scenarios are more pronounced during the winter day, where potential savings are larger, while the difference is smaller on the summer day. Given the greater opportunity for cost savings during the winter months, we will focus on winter days in further analysis, especially when exploring different battery system configurations.

6.3.1.2 Battery System Configuration Comparisons

In this section, we extend the previous analysis by evaluating how potential future RESS impact cost outcomes and charging behaviors, focusing on the winter day. We compare the RESS trajectories and their corresponding costs for Future Battery System A and Future Battery System B, assessing how these configurations influence the BEV trajectories as well.

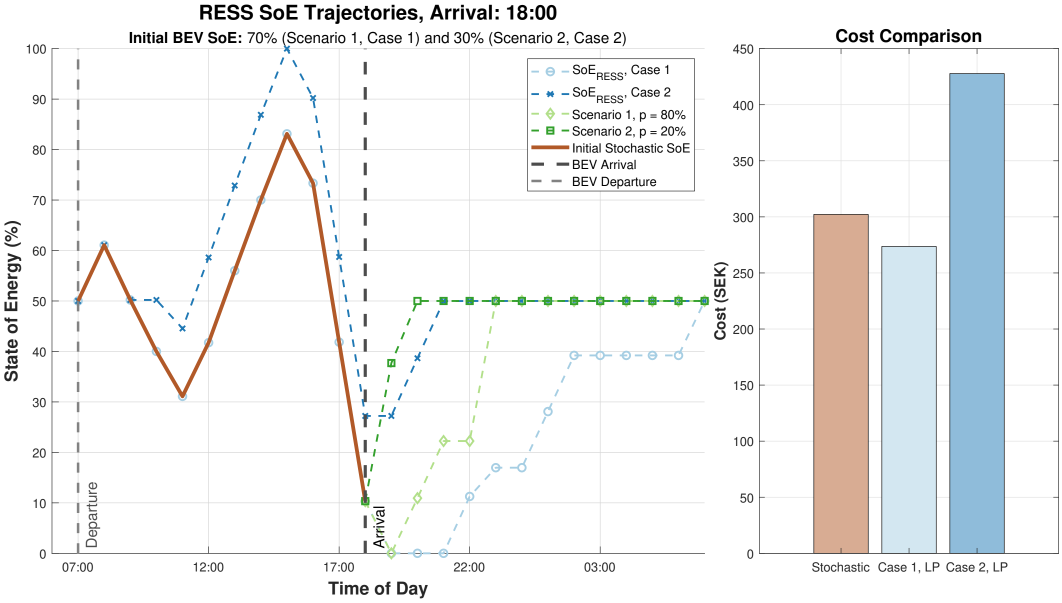

(a) RESS SOE trajectories and cost comparison for a winter day (5 Jan 2024), using Future System A (50 kWh). The BEV arrives at 18:00 and leaves at 7:00 with a target SoE of 80%. Scenario 1 assumes a BEV arrival SoE of 70%, while Scenario 2 assumes 30%.

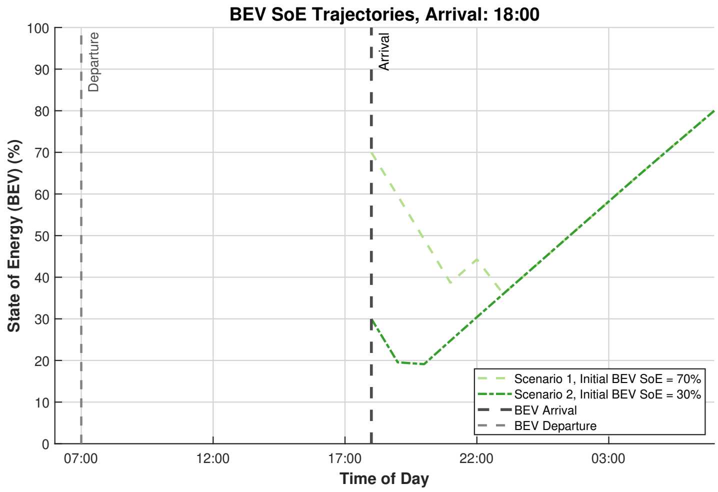

(b) BEV SOE trajectories for the same winter day using Future System A (50 kWh). The BEV arrives at 18:00 and leaves at 7:00 with a target SoE of 80%. Scenario 1 assumes a BEV arrival SoE of 70%, while Scenario 2 assumes 30%.

Figure 6.9: SOE trajectories of the RESS and BEV for a winter day (5 Jan 2024) under Future System A (50 kWh), with two different BEV arrival SoE scenarios.

In Figures 6.9a and 6.9b, we reproduce the winter-day (5 Jan 2024) RESS and BEV trajectories from Figures 6.7a and 6.7b, respectively, but now with a larger 50 kWh home battery (System A).

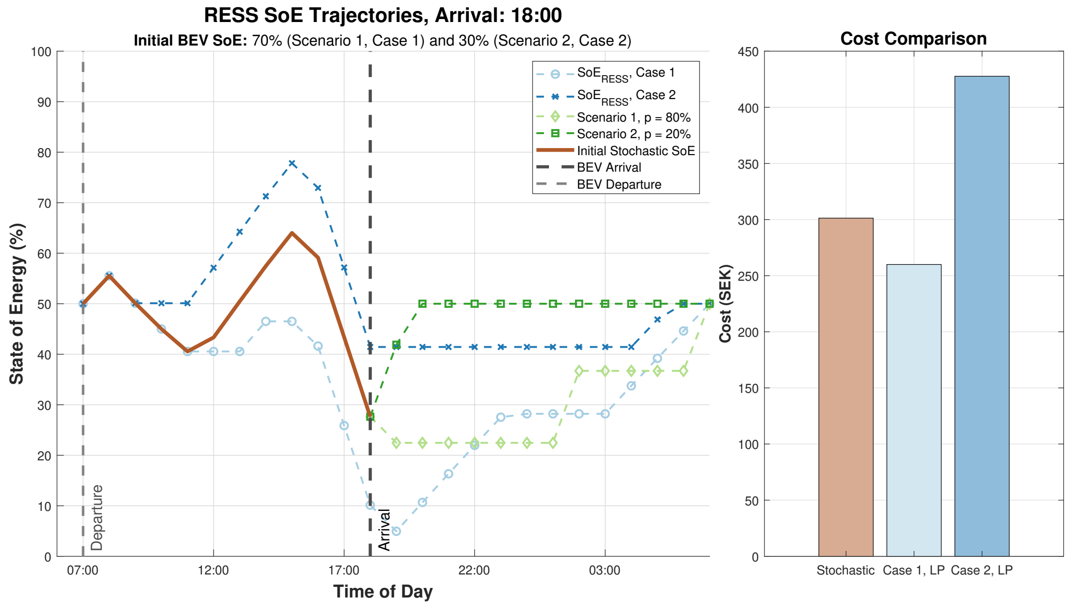

(a) RESS SOE trajectories and cost comparison for a winter day (5 Jan 2024), using Future System B (100 kWh). The BEV arrives at 18:00 and leaves at 7:00 with a target SoE of 80%. Scenario 1 assumes a BEV arrival SoE of 70%, while Scenario 2 assumes 30%.

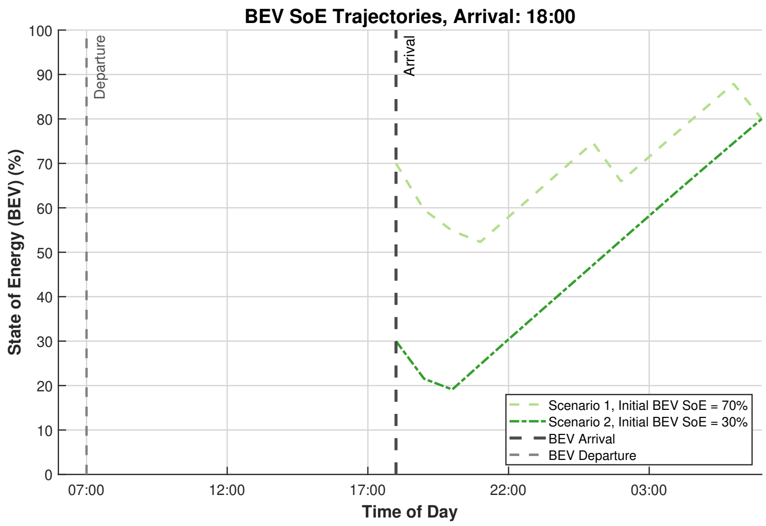

(b) BEV SOE trajectories for the same winter day using Future System B (100 kWh). The BEV arrives at 18:00 and leaves at 7:00 with a target SoE of 80%. Scenario 1 assumes a BEV arrival SoE of 70%, while Scenario 2 assumes 30%.

Figure 6.10: SOE trajectories of the RESS and BEV for a winter day (5 Jan 2024) under Future System B (100 kWh), with two BEV arrival SoE scenarios.

In Figures 6.10a and 6.10b, we reproduce the winter-day (5 Jan 2024) RESS and BEV trajectories from Figures 6.7a and 6.7b using a 100 kWH home battery (System B).

Figures 6.9 - 6.10 confirm that increasing battery capacity lowers costs across all methods. However, the cost reduction is more significant when moving from a typical current battery system to Future Battery System A, while the difference between Future Battery System A and B is smaller.

Another notable difference is in the initial charging behavior during the initial stage, before BEV arrival. With the typical current battery system, the stochastic method closely followed the linear cases. In contrast, for the larger battery systems, the stochastic optimization behaves more dynamically, balancing between the two deterministic cases.

Further examples demonstrating the optimization's functionality with three distinct scenarios are presented in Appendix A.2.2, highlighting the method's scalability and flexibility in handling multiple scenarios.

6.4 Case study

So far, we cannot draw definitive conclusions about the differences between the methods or how comparable they are. To better understand their performance, we must examine what happens when a stochastic approach is not used, relying instead on the LP method, which assumes perfect foresight. In reality, if the car behaves differently than expected and returns with a different SOE than predicted, this assumption breaks down, potentially leading to suboptimal results.

To conduct this analysis, we will perform calculations over several months to evaluate the impact of daily prediction errors and compare the results with the stochastic method that accounts for uncertainty. This will be done for different months of the year to assess variations between winter and summer. Additionally, we will investigate whether certain days lead to significantly higher costs and identify potential patterns in these occurrences.

A wrong prediction happens when we expect the car to arrive with a specific SOE level, but it actually arrives with a different one. In this context, it means planning based on the assumption that the car will return with 70%, only to find that it actually arrives with 30%, forcing us to redo the optimization.

Figure 6.11 show the result for the winter month November to March. The figure shows the difference between the LP method in the two different scenarios, compared with the cost for the LP method with the wrong approximation of the arrival BEV SOE.

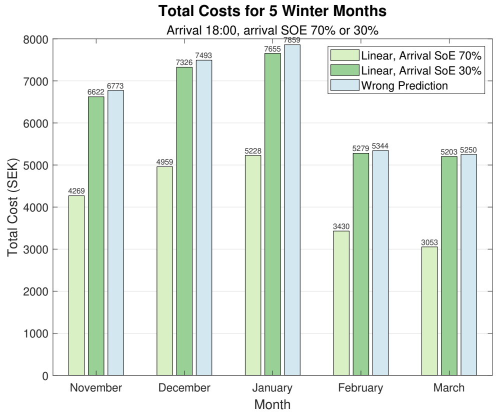

Figure 6.11: Costs LP 2 scenarios and LP wrong assumption over 5 winter month.

The plots clearly show that using only LP and making an incorrect prediction results in higher costs compared to planning for the worst-case scenario. The light green bar represents the cost when the car is correctly assumed to arrive home with 70% state of energy, while the dark green shows the case when the car correctly arrives with 30%. The blue bar illustrates the scenario where we assume the car will arrive with 70%, but it actually arrives with only 30%.

The plot illustrates that making an incorrect assumption about a favorable scenario leads to higher costs than simply planning for a less favorable one from the start. This indicate that relying on a wrong prediction increases cost, highlighting the value of a stochastic approach that accounts for uncertainty in the optimization.

The same trend are true for all months.

6.4.1 Extreme days

The graph above highlight the cost variations across different LP scenarios. However, our primary objective is to compare these results with those of the stochastic method. To better understand the significance of this comparison, it is useful to first identify when extreme days occur. We define extreme days as those on which an incorrect assumption produces the largest cost impact. This will allow us to assess whether the observed cost differences are primarily a result of extreme days or whether the stochastic method consistently outperforms the linear approach across all days, regardless of external conditions.

Table 6.1 presents the 10 most extreme days during the winter months November to Mars, ranked in descending order from the most extreme day.

Table 6.1: Top 10 days with the largest recorded differences, winter.

Date
05-Jan-2024
01-Dec-2023
30-Nov-2023
28-Nov-2023
29-Nov-2023
05-Dec-2023
02-Dec-2023
25-Nov-2023
03-Dec-2023
11-Jan-2024

Table 6.2 presents the 10 most extreme days during the summer months May to September, ranked in descending order from the most extreme day.

Table 6.2: Top 10 days with the largest recorded differences, summer.

Date
08-May-2024
07-May-2024
06-May-2024
12-Jun-2024
11-Jun-2024
17-Jun-2024
13-Jun-2024
16-Jun-2024
09-Jul-2024
21-Jun-2024

6.4.2 Stochastic vs wrong assumption

To conclude our analysis of the stochastic method's performance, we compare three representative cases that demonstrate how different approaches handle uncertainty in the BEV's arrival SOE:

- **Case 1: Perfect foresight (deterministic benchmark)** – This scenario assumes full knowledge of the BEV's arrival SOE in advance. The system knows exactly which days the car will return with 70% or 30% SOE and can therefore plan the entire charging schedule optimally. While unrealistic in practice, this serves as an upper bound on performance.

- **Case 2: Stochastic optimization with re-optimization** – In this more realistic case, uncertainty is explicitly modeled using a stochastic formulation. The first-stage decisions are made based on a probability distribution (e.g., 80% chance of 70% SOE, 20% of 30%). Once the actual SOE is revealed at arrival, a second-stage linear re-optimization is performed with full knowledge of all system parameters.
- **Case 3: Incorrect deterministic assumption** – This approach assumes a fixed (best-case) arrival SOE of 70%, ignoring uncertainty. If this assumption turns out to be wrong (i.e., the car arrives with 30% SOE), a re-optimization must be performed to adjust the plan. This case highlights the potential cost of incorrect assumptions and overconfidence in forecasts.

6.4.2.1 Stochastic vs wrong assumption with the most extreme days - winter

In Figure 6.12, we compare the three optimization cases under an intentionally challenging scenario. Specifically, we assume that the 20% probability of the BEV arriving with a low state of energy (30% SOE) is realized exclusively on the most extreme days, those with high electricity prices or increased demand, as identified in section 6.4.1 .

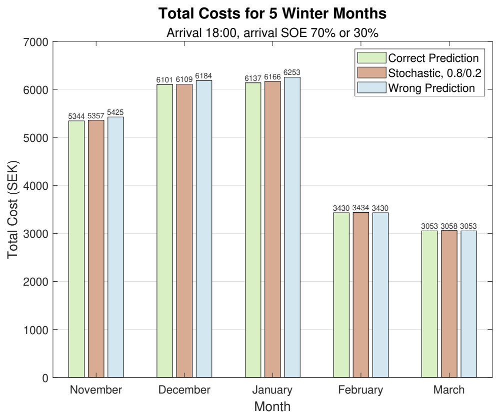

Figure 6.12: Cost stochastic method vs LP wrong assumption with only 20% wrong assumption (extreme days) over 5 winter month (November-Mars).

The figure displays the total energy costs over the winter period (November to March) for each method. The green bars represent the deterministic LP method with perfect foresight, where the actual arrival SOE (30% or 70%) is known in advance. The red bars correspond to the stochastic method, which incorporates uncertainty by optimizing based on weighted probabilities (80% for 70%, 20% for 30%) and re-optimizing the second stage upon realization. The blue bars show the outcome of assuming a 70% SOE at all times, even when the BEV actually arrives with 30%, representing a case of incorrect prediction followed by re-optimization.

Over the five winter months, the total energy costs for each method shown in Figure 6.12 are:

- **LP (correct forecast):** 24 065 SEK
- **Stochastic optimization:** 24 124 SEK (+ 59 SEK vs. LP correct)
- **LP (incorrect forecast):** 24 345 SEK (+ 280 SEK vs. LP correct)

These results demonstrate that even when incorrect assumptions occur only 20% of the days, targeted to the most extreme ones, the resulting cost increase is significant, although not very large over 5 months. While the LP method with perfect foresight yields the lowest cost, it relies on assumptions that are unrealistic in practice.

6.4.2.2 Stochastic vs wrong assumption with the most extreme days - summer

Figure 6.13 shows the same comparison as in the winter case (Figure 6.12), but for the summer months from May to September.

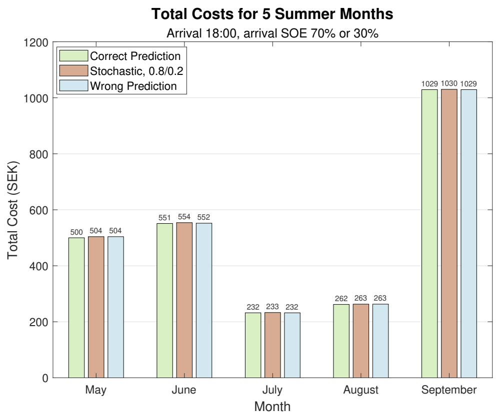

Figure 6.13: Cost stochastic method vs LP wrong assumption with only 20% wrong assumption (extreme days) over 5 summer month (May-Sep)

While the same general trend holds, where the stochastic method performs better than the LP approach with incorrect forecasts, cost differences are significantly smaller during summer:

- **LP (correct forecast):** 2 574 SEK
- **Stochastic optimization:** 2 584 SEK (+10 SEK vs. LP correct)
- **LP (incorrect forecast):** 2 580 SEK (+6 SEK vs. LP correct)

These minor discrepancies reflect lower electricity costs and more stable pricing in the summer, which reduce the consequences of being wrong. Interestingly, the stochastic method is slightly more expensive than the LP with incorrect forecasts in this case. This may be because the LP approach, with its fixed assumptions, is more aggressive in selling excess solar energy back to the grid, maximizing short-term profits. In contrast, the stochastic method takes a more cautious approach, hedging between possible arrival SOEs to ensure feasibility under uncertainty. This cautiousness slightly reduces the opportunity for profit in summer, but the very small difference over five months is insignificant.

6.4.2.3 Stochastic vs wrong assumption with random days

Having examined the impact of incorrect predictions on the most extreme days, we now consider a more realistic scenario where mispredictions are randomly distributed across the five winter months. Since the affected days differ in each run, outcomes may vary depending on which days are incorrectly forecasted. To mitigate this variability, we repeat the analysis 20 times and plot the mean results.

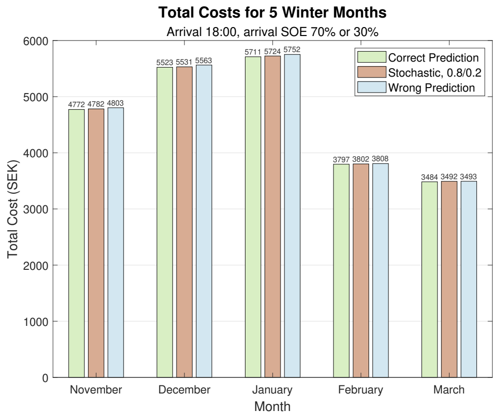

Figure 6.14: Cost stochastic method vs LP wrong assumption with only 20% wrong assumption (random days) over 5 winter month. Average of 20 runs

In the above plot, we see the same three scenarios as before: the deterministic LP method with perfect foresight (green), the stochastic optimization with corresponding probabilities (red), and the deterministic LP method with an incorrect SOE assumption (blue). The results, averaged across 20 runs with randomly chosen incorrect days, confirm the previously observed trends.

The total energy costs over the five winter months are:

- **LP (correct forecast):** 23 287 SEK
- **Stochastic optimization:** 23 331 SEK (+44 SEK vs. LP correct)
- **LP (incorrect forecast):** 23 424 SEK (+137 SEK vs. LP correct)

Taken together, Figures 6.12–6.14 highlight that incorrect SoE assumptions can noticeably impact energy costs, even when mispredictions occur on random days. While the effect is minimal during summer, winter months show that the stochastic method consistently outperforms the naive best-case assumption, offering greater resilience regardless of when prediction errors occur.

6.5 Demand-Charge Tariffs

Finally, we extend the original setup by introducing a Demand-Charge Tariff (DCT) to examine its impact on the charging behavior of both the BEV and RESS. Specifically, our objective is to determine whether the presence of a cost associated with peak power usage influences the overall pattern of electricity consumption from the grid. We conclude the section with a comparative cost analysis, evaluating the difference between incorporating the tariff directly into the optimization process versus applying the tariff cost retrospectively.

To assess the effect of different levels of DCTs, we introduce two tariff penalty levels, referred to as a *low tariff* and a *high tariff*. As described in Section 5.2, we apply a constant flat-rate penalty throughout the day based on the daily peak power consumption. This penalty is scaled using the tariff coefficient ω in Equation (5.20). In the low tariff scenario, we set $\omega = 1.5$, representing a modest and more realistic penalty (in SEK/kW). In contrast, the high tariff scenario uses a significantly larger and unrealistic value of $\omega = 50$, representing an extreme case. Albeit unrealistic, this high tariff setup allows us to examine whether stronger penalties lead to notable changes in consumption patterns compared to more moderate pricing.

6.5.1 BEV/RESS Trajectories with Demand-Charge Tariffs

We begin by examining how the charging trajectories changes for the BEV and the RESS when tariffs are introduced. In the following plots, we compare the original optimization results with those obtained when tariffs are taken into account. Both LP and stochastic optimization methods are analyzed under scenarios with high and low tariffs, applied to both the Current Battery System and the Future Battery System A (50kWh). We first present the results from the LP optimization:

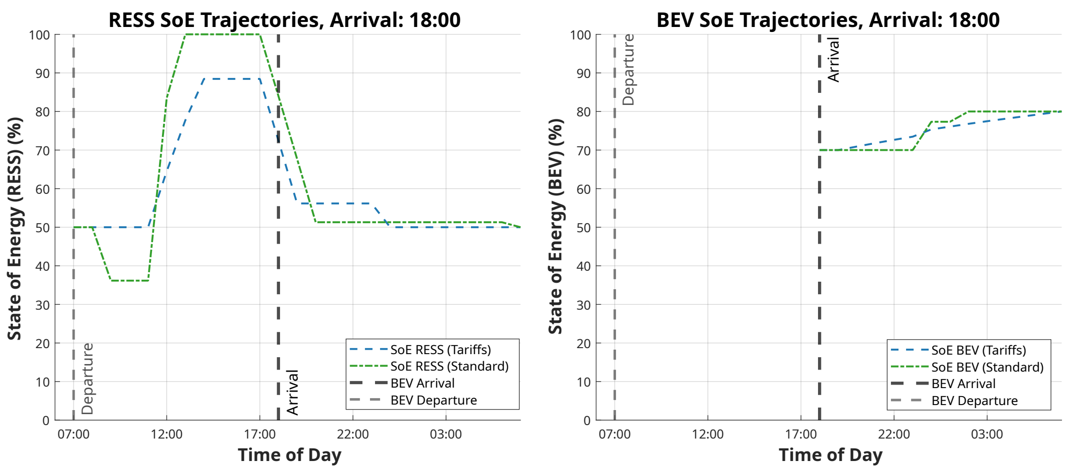

Figure 6.15: Linear optimization for a 20 kWh battery comparing low-tariff and no-tariff scenarios, with the BEV trajectory on the right and the RESS trajectory on the left.

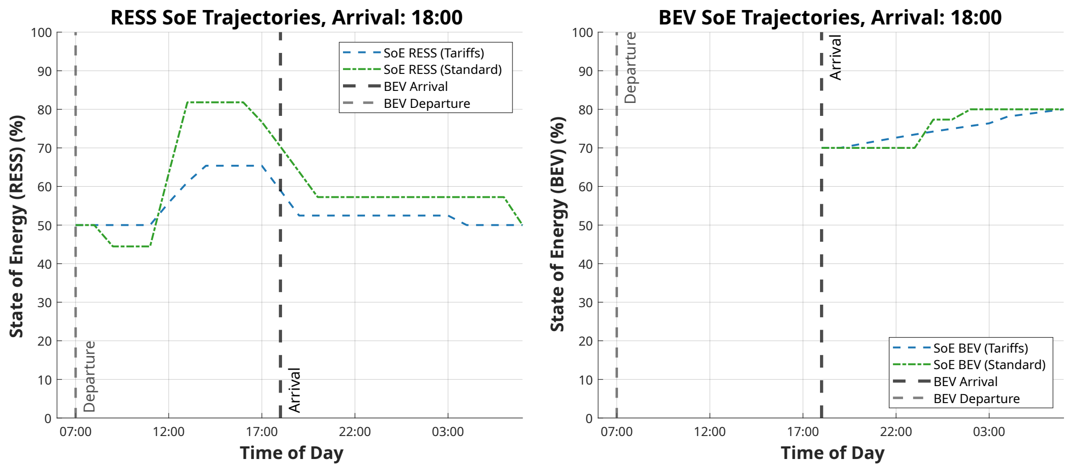

Figure 6.16: Linear optimization for a 50 kWh battery comparing low-tariff and no-tariff scenarios, with the BEV trajectory on the right and the RESS trajectory left.

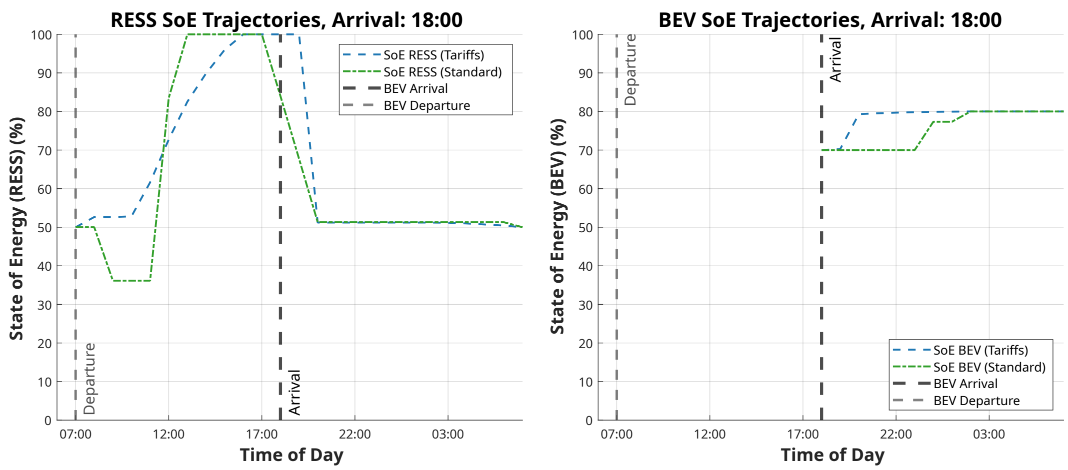

Figure 6.17: Linear optimization for a 20 kWh battery comparing high-tariff and no-tariff scenarios, with the BEV trajectory on the right and the RESS trajectory on the left.

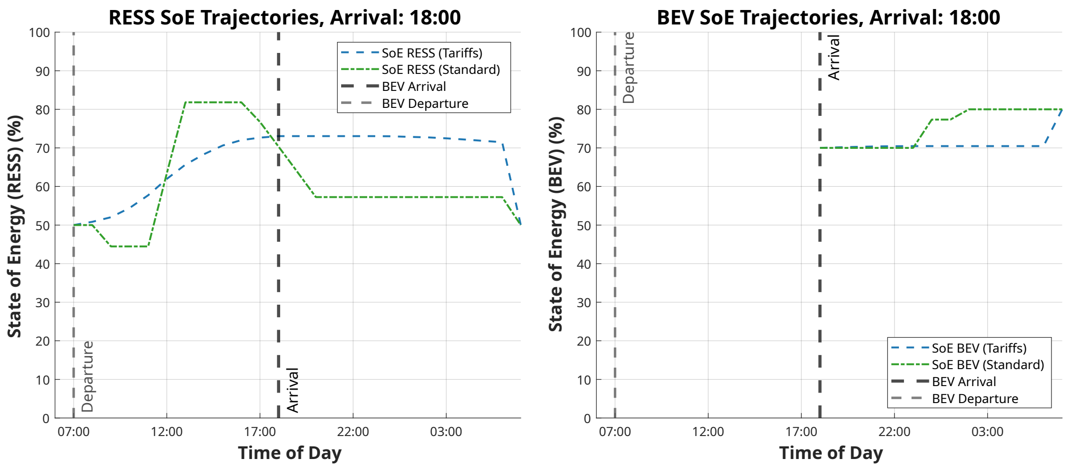

Figure 6.18: Linear optimization for a 50 kWh battery comparing high-tariff and no-tariff scenarios, with the BEV trajectory on the right and the RESS trajectory on the left.

On the left side, we see the RESS charging trajectory, and on the right, the BEV charging trajectory. The car arrives home at 18.00 and departs at 07:00. The blue line represents the optimization with tariffs included, while the green line shows the case without tariffs. As seen in the plots, the trajectory with tariffs is a bit more stable and tends to avoid large peaks. A notable difference is that, with tariffs, the RESS is used to charge the BEV, something not observed in the optimization without tariffs.

These patterns are consistent across the figures 6.15 - 6.18, which show the results from the LP optimization under different conditions: low and high tariffs, as well as different battery system configurations. Despite these variations, the general behavior remains similar, highlighting how the presence of tariffs influences the system's strategy in a consistent way.

Having reviewed the LP optimization outcomes, we now turn to the stochastic optimization results seen in Figures 6.19–6.22.

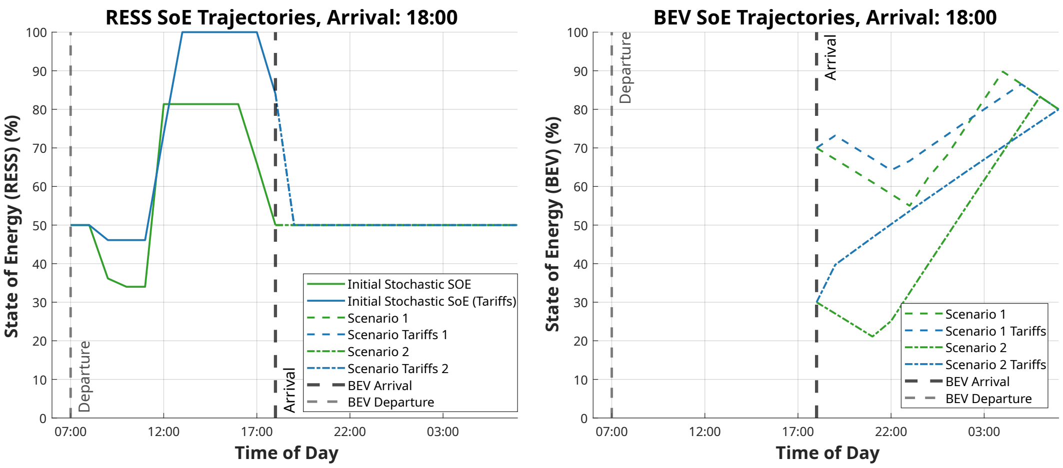

Figure 6.19: Stochastic optimization for a 20 kWh battery comparing low-tariff and no-tariff scenarios, with the BEV trajectory on the right and the RESS trajectory on the left.

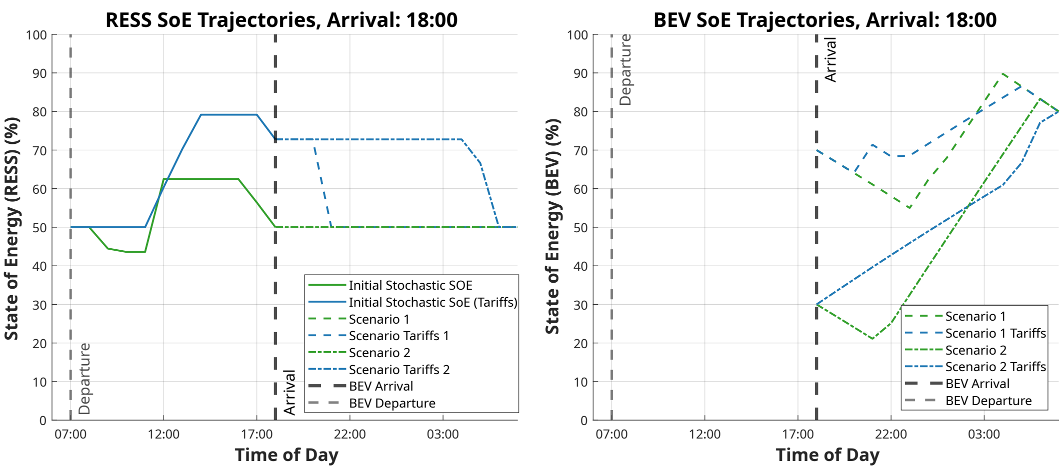

Figure 6.20: Stochastic optimization for a 50 kWh battery comparing low-tariff and no-tariff scenarios, with the BEV trajectory on the right and the RESS trajectory on the left.

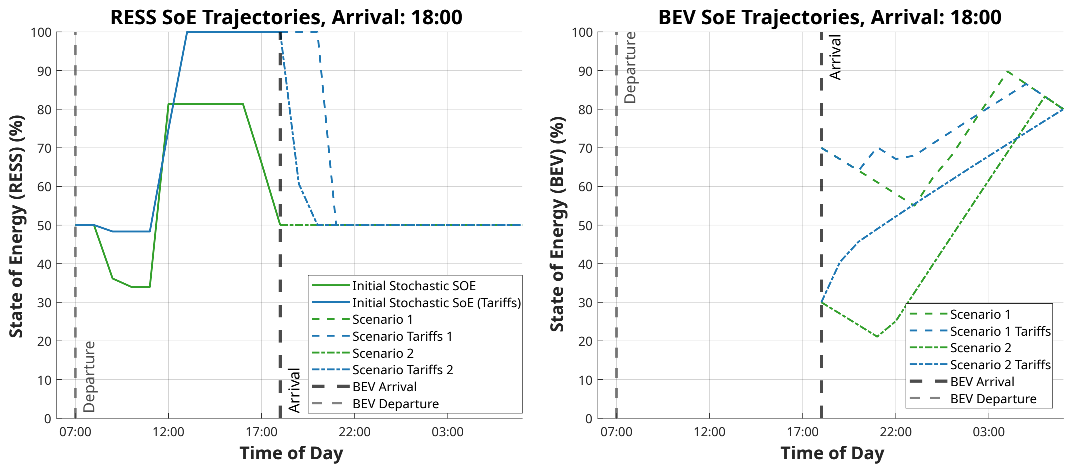

Figure 6.21: Stochastic optimization for a 20 kWh battery comparing high-tariff and no-tariff scenarios, with the BEV trajectory on the right and the RESS trajectory on the left.

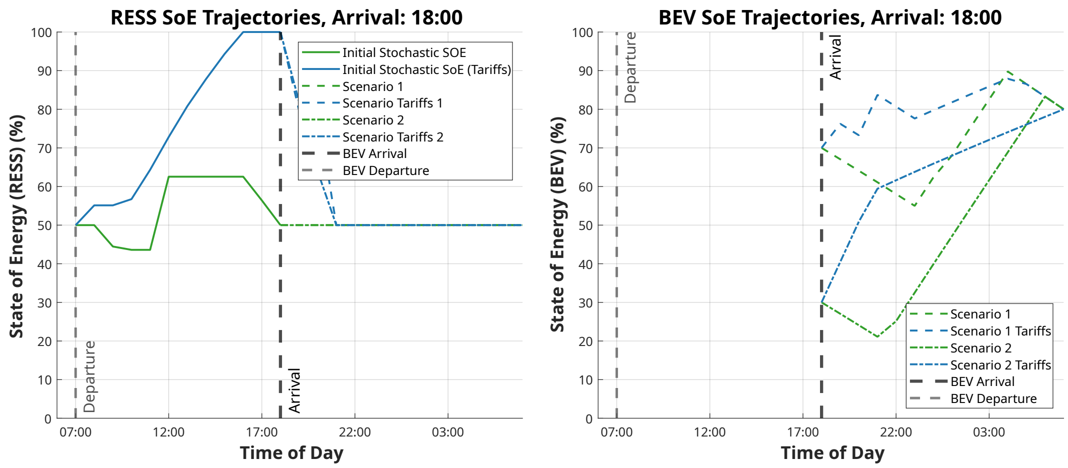

Figure 6.22: Stochastic optimization for a 50 kWh battery comparing high-tariff and no-tariff scenarios, with the BEV trajectory on the right and the RESS trajectory on the left.

On the left side of each figure, we display the RESS SOE. Since we are now solving a two-stage stochastic problem, each figure includes two pre-arrival trajectories, one green (without tariffs) and one blue (with tariffs), as well as four post-arrival trajectories: two green (no-tariff realizations) and two blue (tariff realizations). These additional post-arrival curves reflect the uncertainty in the BEV's SOE at the time of arrival (18:00), which requires the optimization process to account for multiple possible outcomes and adapt charging or discharging accordingly.

On the right side of each figure, the corresponding BEV charging profiles are shown, following the same color scheme and structure. Across both RESS and BEV plots, the inclusion of tariffs (blue curves) results in noticeably smoother charging behavior with reduced peak power usage.

Figures 6.19–6.22 show that introducing DCTs fundamentally reshapes the charging trajectories for both the BEV and the RESS. When tariffs are included, the power trajectories become noticeably smoother, with lower peaks, as the optimizer tries to avoid large simultaneous purchases to keep tariff costs down. The plots also reveals that the RESS now discharges to supply the BEV with electricity, a behavior that was not seen when tariffs were not included.

6.5.2 Electricity from the grid

Previous figures focus on the RESS and BEV charge and discharge patterns but do not directly reveal the grid-draw peaks that drive the DCT. To make those peaks explicit, we plot only the grid electricity import trajectories for our stochastic scenarios, considering both 20 kWh and 50 kWh RESS capacities under low- and high-tariff structures.

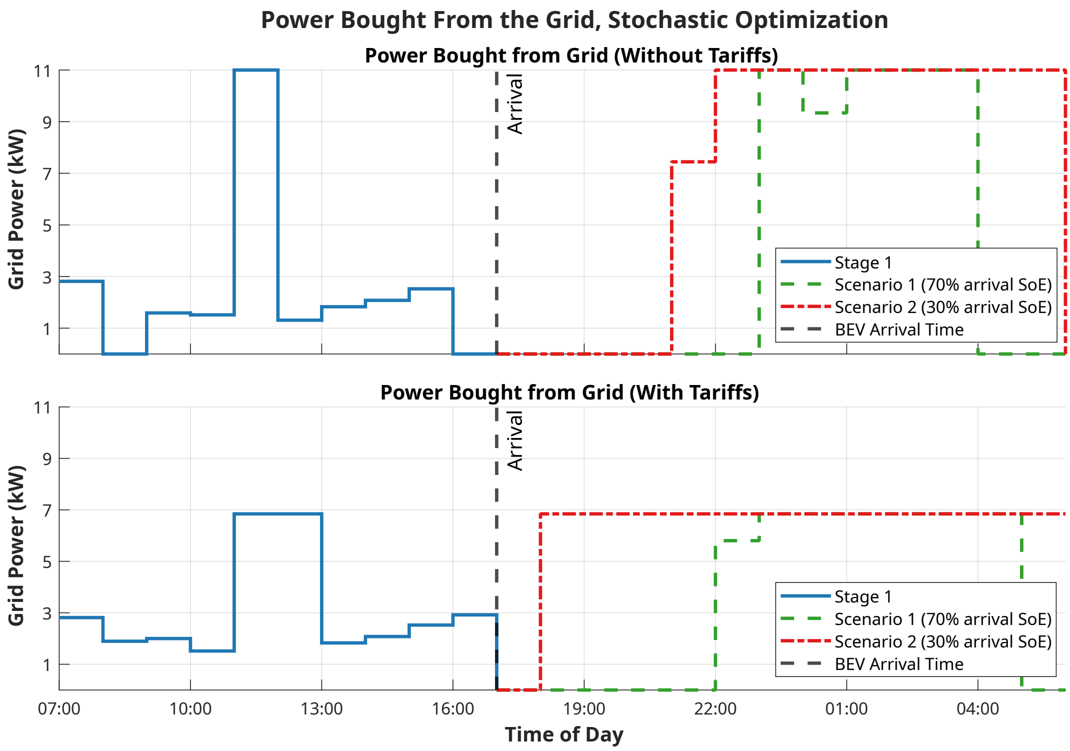

Figure 6.23: Electricity purchased from the grid over one day under stochastic optimization without tariffs vs with low tariffs, using a 20 kWh RESS

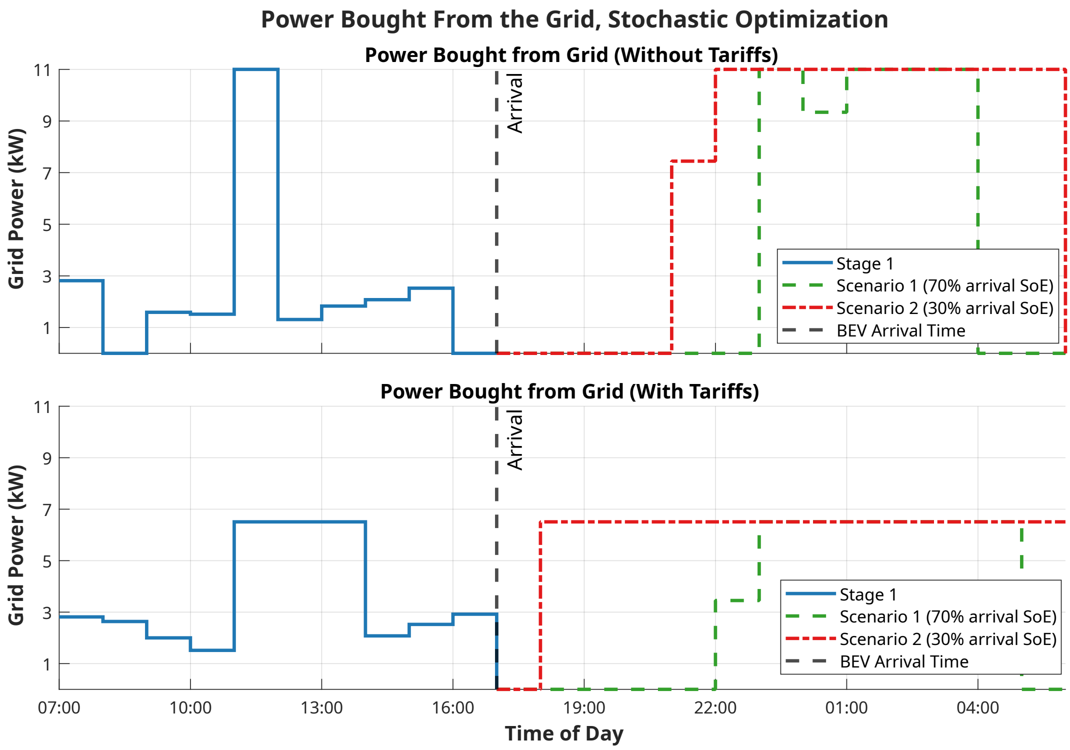

Figure 6.24: Electricity purchased from the grid over one day under stochastic optimization without tariffs vs with high tariffs, using a 20 kWh RESS

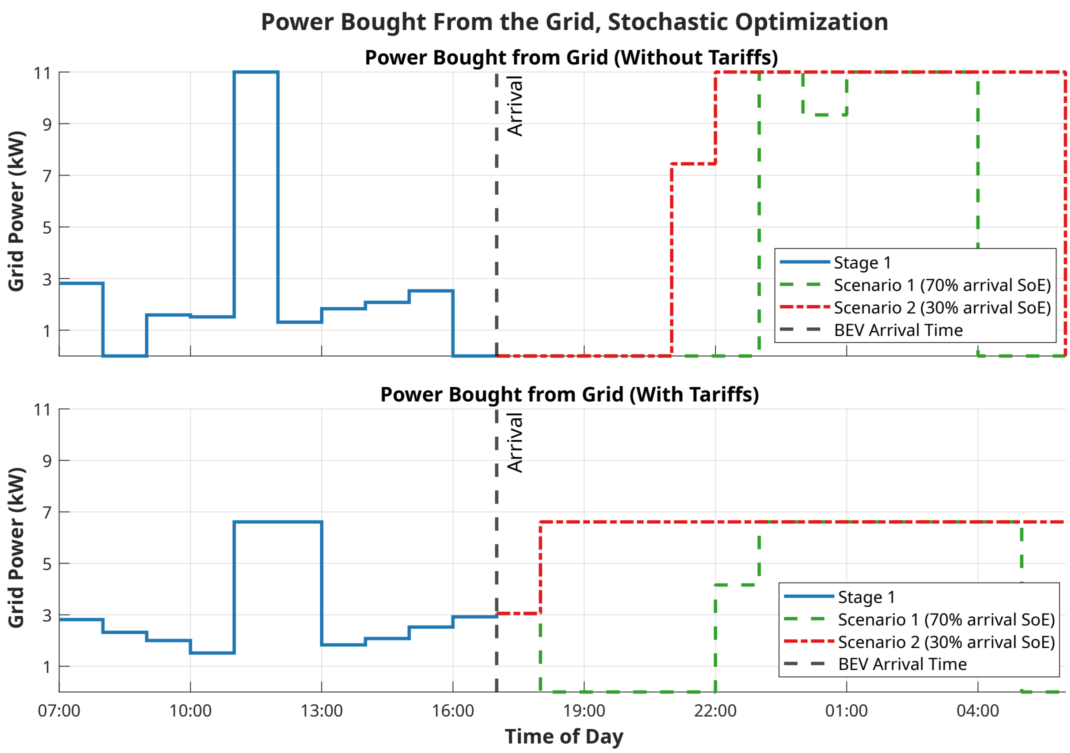

Figure 6.25: Electricity purchased from the grid over one day under stochastic optimization without tariffs vs with low tariffs, using a 50 kWh RESS

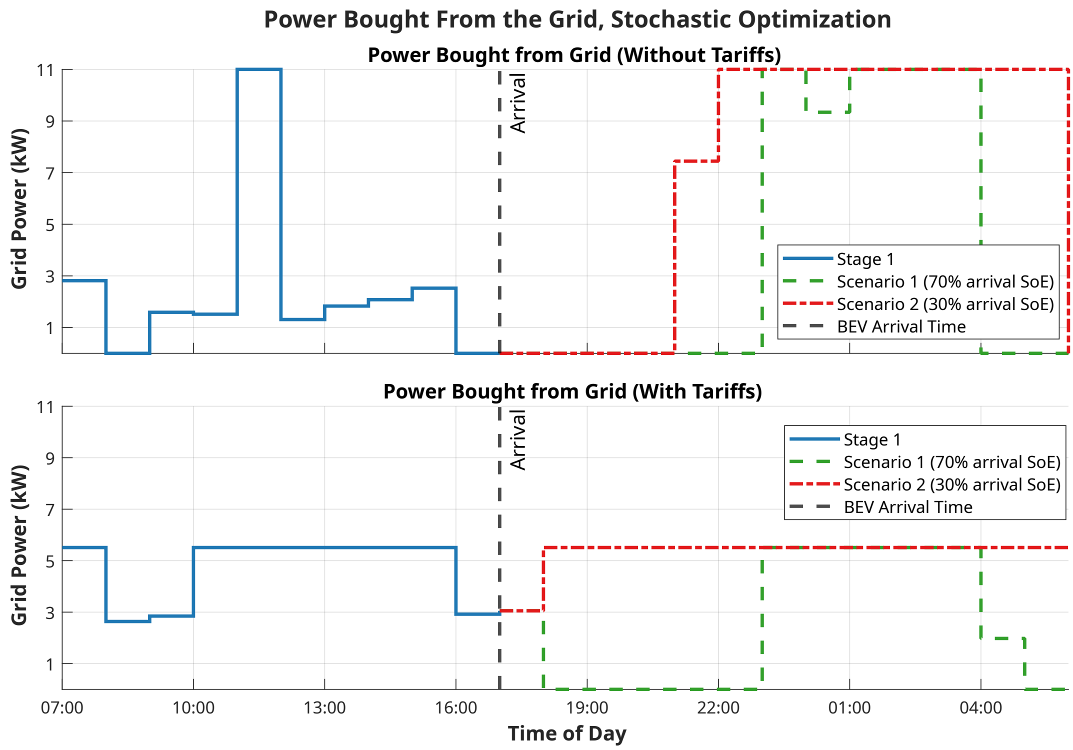

Figure 6.26: Electricity purchased from the grid over one day under stochastic optimization without tariffs vs with high tariffs, using a 50 kWh RESS

The plots show the trajectory of the amount of electricity purchased at each time step. The blue curve represents imports prior to the BEV's return at 18:00. After arrival, two trajectories appear: the green curve corresponds to a 70 % initial BEV SOE, and the red curve to a 30 % SOE.

The analysis of DCTs reveals clear changes in the power drawn from the grid. Without any DCT, the optimization frequently utilizes the system's maximum allowable power draw of 11 kW, where no incentive exists to limit peak demand. However, once DCTs are introduced, peak power usage is significantly reduced, even under modest tariff levels.

Interestingly, increasing the tariffs from low to high had only a marginal effect on peak reduction in both battery setups. This suggests that the low tariff already enforces peak reduction close to what is technically feasible given the system's operational constraints. The optimization must still ensure that the BEV and RESS reaches their target SOE within the time frame, which imposes a lower bound on the achievable peak.

However, the larger battery consistently achieves lower peaks compared to the smaller one, due to its greater storage capacity and flexibility in shifting loads. Moreover, while the high tariff does slightly reduce the peak further in the larger battery scenario, the gain is modest.

6.5.3 Tariff Cost Comparison

We conclude by comparing total system costs under two different approaches:

1. **Integrated-tariff optimization**: DCTs are included in the HEMS objective from the outset, guiding dispatch and storage decisions to minimize both energy and peak-demand charges.
2. **Post-hoc tariff application**: The HEMS performs a standard cost minimization without considering tariffs, after which peak-demand charges are calculated separately and added to the total cost.

This comparison highlights how explicitly accounting for tariffs within the optimization process influences peak demand mitigation and overall operating expenses.

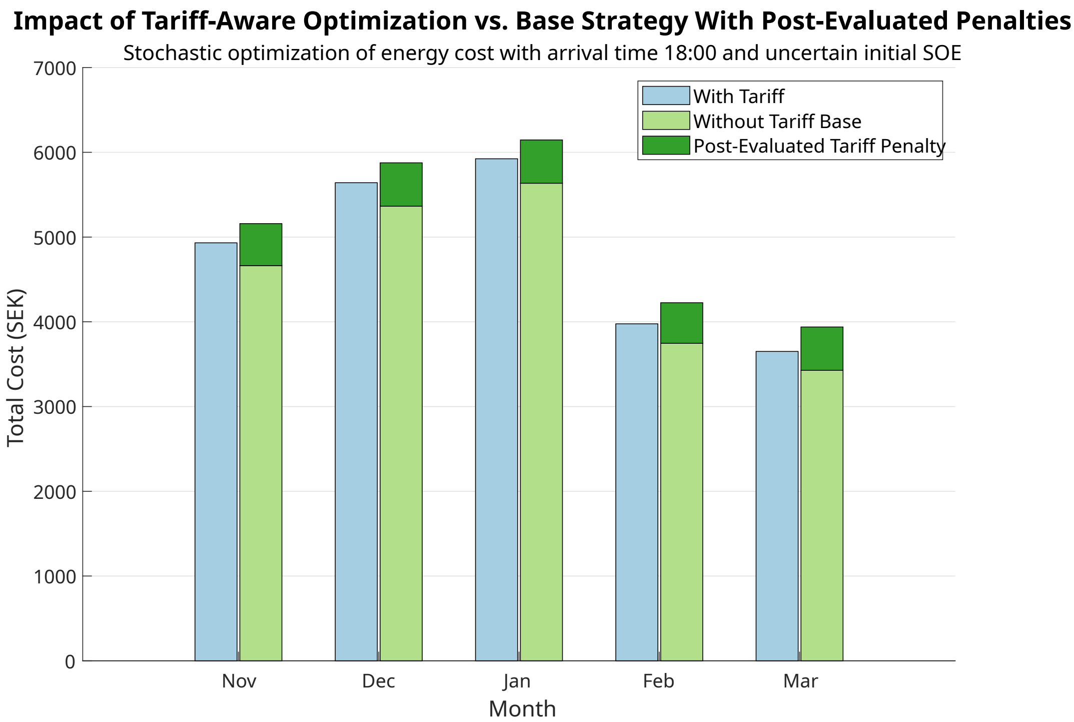

Figure 6.27: Total System Cost Comparison: Integrated low Tariff Optimization vs. Post-hoc low Tariff Application over 5 winter month

The plot 6.27 illustrates the total system cost comparison between integrated-tariff optimization and post-hoc tariff application over the five winter months (November–March). The blue bars represent costs when tariffs are integrated into the HEMS optimization, while the light green bars show the baseline optimization cost without tariffs and the dark green segments indicate the additional tariff charges applied afterward. In each of the five months, the combined light and dark green bars exceed the blue bars, highlighting the benefit of including tariffs directly in the optimization.

7

Conclusion & future research

In this final section, we summarize the key findings from our study and reflect on the practical implications of the results. We begin by drawing general conclusions, followed by direct answers to the research questions posed at the start of the thesis. Finally, we highlight a few potential directions for future research that could further explore and expand upon the work presented in this thesis.

7.1 Conclusion

What we can conclude is that our results show that planning for uncertainty outperforms conventional Linear Programming (LP) with full foresight followed by re-optimization upon vehicle arrival. The same goes when we include Demand-Charge Tariffs (DCT). Although the stochastic approach is slightly more complex than a basic LP, it is still manageable. While the stochastic method introduces some added complexity, it remains highly manageable. Just adding a few scenarios provides a more robust and realistic solution, with minimal increase in programming effort or any noticeable impact on computation time.

The average annual cost savings for a single household are relatively small, around 250 SEK, but the potential impact scales in collective settings. For example, in applications like fleet management, shared residential energy communities, or commercial car pools, where many BEVs operate under the same optimization framework, the aggregated savings become substantial. A fleet of 100,000 vehicles following this approach could for example yield savings of up to 25 million SEK per year.

Beyond the financial gains, this smarter scheduling contributes to a more sustainable and resilient energy system. Charging is shifted toward hours with lower spot prices, which tend to align with periods of cleaner energy production. Moreover, the ability to sell back to the grid improves flexibility and supports grid stability. Crucially, by reducing peak loads through coordinated energy use, this approach helps alleviate stress on the power grid, delaying or even avoiding costly infrastructure upgrades and enabling the grid to accommodate more BEVs without immediate expansion.

7.1.1 Research Questions

Given an uncertainty, how does it change the formulation of the objective function of the HEMS?

The formulation of the objective function in the stochastic model differs from that of the LP model, depending on the type of uncertainty considered. If the uncertainty lies in the car's SOE or its arrival time, the stochastic model retains the same objective function, and modifications are made in the constraints (see 5.13). However, if the uncertainty are regarding to the electricity prices, the objective function must also be reformulated, as shown in the appendix (A.1).
Can you get a lower energy cost with another optimization method, such as stochastic optimization?

If we have perfect foresight, knowing every parameter including the car's exact SOE at arrival, stochastic optimization cannot outperform linear optimization in terms of cost. However, in reality, we cannot predict the future, and the arrival SOE is unknown in advance. The LP method must assume a single SOE value, which often turns out to be inaccurate. In contrast, a stochastic approach treats the SOE as uncertain, plans for a range of possible values, and therefore achieves a lower actual cost in practice.

How sensitive is the optimal solution that has been conducted as a LP-problem to uncertainties in the variables?

The LP method is sensitive to uncertainty, as illustrated in Figures 6.11–**??**. Because it assumes perfect knowledge of future conditions, any deviation from those assumptions forces the system to respond reactively, often recharging during peak price hours, which leads to higher electricity costs.

Does an uncertainty in the variables, e.g. time of arrival and difference in the cars state of energy, have a impact on the optimal solution?

In Chapter 6.2, the plots show that varying the BEV's arrival time has minor impact on overall cost. Although we observed a small effect for 20 kWh home batteries, that sensitivity disappears for 50 kWh and 100 kWh systems, particularly over a 100-day horizon. As a result, we decided not to pursue further analysis of uncertainties in arrival time in our DESP implementation.

Uncertainty in arrival time has little effect on total cost, but variability in the vehicle's SOE at arrival does have a noticeable impact. The key takeaway is that it is better to account for the risk of a low arrival SOE during optimization than to assume a high arrival SOE and occasionally face higher costs when that assumption turns out to be incorrect. This cost difference is most pronounced on "extreme" days, though it remains present even under typical conditions. In summer, however, the impact is minimal due to lower home loads and greater solar availability.

In conclusion, uncertainty does alter the optimal solution. While the effect on total minimized cost may vary, the charging schedule is always affected.

With the uncertain variables, how will the charge/discharge levels of energy change for the BEV and RESS?

The charge and discharge patterns of the RESS and BEV change depending on the type of uncertainty being addressed. In the stochastic model, the RESS adjusts its charge level in stage 1 to prepare for the full range of possible BEV arrival SOE scenarios. After the BEV arrives and its actual SOE is revealed, it is then charged accordingly in stage 2. This behavior is illustrated in the figures in Section 6.3.

How do demand-charge tariffs influence the charging trajectories of the BEV and RESS, and is it beneficial to include them in the optimization?

Including tariffs in our model changes both the BEV and RESS trajectories. With tariffs in place, the system follows a smoother profile that avoids large peaks. Another notable difference is that, with tariffs, the RESS is used to charge the BEV, something not observed in the optimization without tariffs.

7.2 Future Research

In the current model, the optimization is performed on a daily basis with many already known parameters. This means that the algorithm makes charging decisions within the span of a single day with given historical data of weather, spot prices etc. While this approach is enough for our reasearch, there are several aspects that could be explored in future research to further improve performance and realism of this problem.

7.2.1 Extended Optimization Horizon

We only looked at 24 hours at a time, but if you were to extend the optimization to cover multiple days, the system would be able to analyze historical pricing patterns and advise the owner accordingly. For example, if the conditions show that today is not the optimal day for charging, the system could notify the user to postpone charging by one or several days. By examining a longer period of time, it is also possible to design tariff models that more closely resemble those used by power grid companies, ensuring a more accurate and realistic pricing forecast.

7.2.2 Additional Scenarios

Our algorithm in Matlab is capable of handling a large number of different scenarios and uncertainties, but for the purpose of this report, we have mainly focused on three types of uncertainty: uncertainty in the arrival SOE, uncertainty in arrival time and uncertainty in electricity prices. So far, we have explored these uncertainties separately. For future research, an interesting idea would be to implement several types of uncertainties at the same time, as well as to include a larger number of scenarios simultaneously.

7.2.3 Handling of Non-feasible Solutions

We did not implement a specific solution for cases where the optimization problem was infeasible. This was not an issue in our study since we primarily worked with arrival SOE levels of 30% and 70%. However, we observed that at lower arrival SOE levels, the optimization can sometimes become infeasible. This is mainly because the system does not have sufficient time to charge the BEV up to the target SOE of 80% before departure.

Although we did not implement a solution for this, we had a few ideas on how it could be handled. One idea is that when the car arrives home and the system detects that it will not be able to reach the target SOE, it automatically lowers the target SOE to something feasible. Another idea would be to adjust the target SOE depending on the arrival level, for example, if the car comes home with less than 25%, it would only charge up to 60%, and if it comes home with more than 25%, it would charge up to 80%.

Otherwise, if the optimization is extended to cover several days, this problem with infeasible solutions would likely disappear, since the system would be able to shift charging to the next day if needed.

7.2.4 Demand-Charge Tariffs

In our implementation, we used a single, constant DCT for every hour and day to demonstrate how the optimization adapts to tariff signals and to highlight the benefits of including tariffs versus ignoring them. While optimizing over a one-month horizon is more realistic, since power-grid companies typically base their rates on monthly usage, focusing on just one day can still be valuable. For more accurate daily modeling, we recommend the approach presented by [8], which adjusts rates depending on the day of the month, providing a more realistic tariff structure than our flat-rate model.

The DCT implementation according to [8] is:

$$\min\ F = \sum_{t \in T} (\lambda_t^{RTD} P_t^{\tilde{h}}) \ + \ \mu \lambda^{DCT} \max\left[(\max\,(p^{\tilde{h}}) - p', 0)\right] \tag{6.1}$$

We have taken inspiration from the equation to implement tariffs to our deterministic stochastic formulation and get the following objective function that could be relevant for future research.

$$c^T x_t \ + \ \sum_{s \in S} p_s\, c_s^T\, y_{t,s} \ + \ \mu\, z \max\left[(\max\,(peak^{day} - peak^{max}, 0)\right] \tag{6.1}$$

where

μ	penalty weight depending on current day d, amount of days D of the current month and the tariff w ($\mu = w \cdot \frac{d}{D}$)
z	tariff cost for each time step t.
$peak^{day}$	peak for the current day d.
$peak^{max}$	highest peak for the current month.

7.2.5 Additional Future research

There a few more things that we did not take into account in our problem that would be interesting to explore in the future. For example, using real-time electricity data, live weather data, and adding a penalty for discharging the car. When we discharge and charge a battery frequently, it affects the battery's lifetime, and it would be worth looking into how much this actually matters. It might turn out that it's not worth discharging the battery just to save a few SEK, because the loss in battery lifetime could be more expensive than the money saved.

Bibliography

[1] Egidio, Leo, Engell, Sebastian. (2018). *Integrated day-ahead energy procurement and production scheduling.* Automatisierungstechnik, 66, 950-963.

[2] Konumenternas Energimarknadsbyrå. (2023). *Normal elförbrukning och elkostnad för villa.* https://www.energimarknadsbyran.se/el/dina-avtal-och-kostnader/elkostnader/elforbrukning/normal-elforbrukning-och-elkostnad-for-villa/

[3] Engergimarknadsinspektionen. (2025). *Effektavgift.* https://ei.se/konsument/el/elnatsavgiften-och-elnatsreglering/effektavgift

[4] Golshannavaz, Sajjad. (2018). *Cooperation of electric vehicle and energy storage in reactive power compensation: An optimal home energy management system considering PV presence.* Sustainable Cities and Society, 39, 317-325.

[5] Hou, Xuan, Wang, Jun, Huang, Tao, Wang, Tao, and Wang, Peng. (2019). *Smart Home Energy Management Optimization Method Considering Energy Storage and Electric Vehicle.* IEEE Access, 7.

[6] Iversen, Emil B., Morales, Juan M., and Madsen, Henrik. (2014). *Optimal charging of an electric vehicle using a Markov decision process.* Applied Energy, 123, 1-12.

[7] Kanakadhurga, Dharmaraj, and Prabaharan, Natarajan. (2024). *Smart home energy management using demand response with uncertainty analysis of electric vehicle in the presence of renewable energy sources.* Applied Energy, 364.

[8] Luo, Fengji, Kong, Weicong, Ranzi, Gianluca, and Dong, Zhao Yang. (2020). *Optimal Home Energy Management System With Demand Charge Tariff and Appliance Operational Dependencies.* IEEE Transactions on Smart Grid, 11(1), 4-14.

[9] Molla, Tesfahun, Baseem, and Singh, Pawan. (2018). *A comprehensive analysis of smart home energy management system optimization techniques.* Journal of Autonomous Intelligence, 1.

[10] Mohammad, Arshad, Zuhaib, Mohd, Ashraf, Imtiaz, Alsultan, Marwan, Ahmad, Shafiq, Sarwar, Adil, and Abdollahian, Mali. (2021). *Integration of Electric Vehicles and Energy Storage System in Home Energy Management System with Home to Grid Capability.* Energies, 14.

[11] Nord Pool. (2025). *Day-ahead prices.* https://data.nordpoolgroup.com/auction/day-ahead/prices?deliveryDate=latest&currency=SEK&aggregation=DeliveryPeriod&deliveryAreas=AT,SE3

[12] Shapiro, Alexander, Philpott, Andy. (2007). *A Tutorial on Stochastic Programming.*

[13] SMHI. (2025). *Års- och månadsstatistik - tabeller för temperatur, vind, nederbörd och solskenstid*. https://www.smhi.se/data/temperatur-och-vind/temperatur/ars--och-manadsstatistik

[14] Thomas, Dimitrios, Deblecker, Olivier, and Ioakimidis, Christos S. (2018). *Optimal operation of an energy management system for a grid-connected smart building considering photovoltaics' uncertainty and stochastic electric vehicles' driving schedule*. Applied Energy, 210, 1188-1206.

A
Appendix

A.1 Additional Implementations:

A.1.1 Uncertainty in Electricity Price

We consider two distinct pricing scenarios: one representing a period of high electricity prices and the other reflecting a period of lower prices and each scenario has the probability p_s to occur. For this implementation, no BEV is included in the HEMS. For uncertainty in electricity price we thus get the objective function for two scenarios from Equation (4.7):

$$\mathcal{J} = \mathbb{c}^T \mathbb{x} + p_1 \mathbb{c}_1^T \mathbb{y}_1 + p_2 \mathbb{c}_2^T \mathbb{y}_2. \tag{A.1}$$

where:

- $\mathbb{c} \in \mathbb{R}^{d_1 \mathcal{T}}$, $\mathbb{c}_1 \in \mathbb{R}^{d_2 \mathcal{T}}$, and $\mathbb{c}_2 \in \mathbb{R}^{d_2 \mathcal{T}}$ are cost vector for the first-stage ($\mathbb{c}$) and second-stage (scenario dependent) decisions ($\mathbb{c}_1$ and $\mathbb{c}_2$),
- $\mathbb{x} \in \mathbb{R}^{d_1 \mathcal{T}}$ is the first-stage decision vector,
- $\mathbb{y} \in \mathbb{R}^{d_2 \mathcal{T}}$ is the second-stage decision vector for scenario s,
- and $\mathcal{T}$ is the number of time steps.

The first-stage decision vector is stacked by variable accross all time steps:

$$\mathbb{x} = \begin{bmatrix} \mathbf{P}_{buy} \\ \mathbf{P}_{sell} \\ \mathbf{P}_{cR} \\ \mathbf{P}_{dR} \\ \mathbf{SOE}_R \end{bmatrix} = \begin{bmatrix} P_{buy}(1) \\ \vdots \\ P_{buy}(\mathcal{T}) \\ P_{sell}(1) \\ \vdots \\ SOE_R(\mathcal{T}) \end{bmatrix}. \tag{A.2}$$

Similarly, the second-stage decision vectors $\mathbb{y}_1$ or $\mathbb{y}_2$ is given by

$$\mathbb{y}_s = \begin{bmatrix} \mathbf{P}^1_{buy} \\ \mathbf{P}^1_{sell} \\ \mathbf{P}^1_{cR} \\ \mathbf{P}^1_{dR} \\ \mathbf{SOE}^1_R \end{bmatrix} = \begin{bmatrix} P^1_{buy}(1) \\ \vdots \\ P^1_{buy}(\mathcal{T}) \\ P^1_{sell}(1) \\ \vdots \\ SOE^1_R(\mathcal{T}) \end{bmatrix}. \tag{A.3}$$

$$\mathrm{y}_s = \begin{bmatrix} \mathbf{P}^2_{buy} \\ \mathbf{P}^2_{sell} \\ \mathbf{P}^2_{cR} \\ \mathbf{P}^2_{dR} \\ \mathbf{SOE}^2_R \end{bmatrix} = \begin{bmatrix} P^2_{buy}(1) \\ \vdots \\ P^2_{buy}(\mathcal{T}) \\ P^2_{sell}(1) \\ \vdots \\ SOE^2_R(\mathcal{T}) \end{bmatrix}. \tag{A.4}$$

Variables $p_1, p_2 \in [0,1]$ are the associated probability for each scenario.

Constraints:

$$P_{solar} = \min\{\eta_{sol} \cdot A_{sol} \cdot I_{sun}(t) \cdot \gamma_{cf}, N_{sol} \cdot P^n_{sol}\} \tag{A.5a}$$
$$P_{home}(t) = P_{base}(t) + P_{heat}(T_{amb}, t) + P_{cool}(T_{amb}, t) \tag{A.5b}$$
$$P_{home}(t) - P_{solar}(t) = P_{sell}(t) - P_{buy}(t) - P_{dR}(t) + P_{cR}(t) \tag{A.5c}$$
$$P^1_{home}(t) + P^1_{solar}(t) = P^1_{sell}(t) - P^1_{buy}(t) - \sum_{b\in\mathcal{B}} \Big(P^1_{d,b}(t) - P^1_{c,b}(t)\Big) \tag{A.5d}$$
$$P^2_{home}(t) + P^2_{solar}(t) = P^2_{sell}(t) - P^2_{buy}(t) - \sum_{b\in\mathcal{B}} \Big(P^2_{d,b}(t) - P^2_{c,b}(t)\Big) \tag{A.5e}$$
$$SOE_R(t+1) = SOE_R(t) + \frac{1}{E_R}(1-\delta) \cdot P_{cR} - \frac{1}{E_R}(1+\delta) \cdot P_{dR} \tag{A.5f}$$
$$SOE^1_R(t+1) = SOE^1_R(t) + \frac{1}{E_R}(1-\delta) \cdot P^1_{cR} - \frac{1}{E_R}(1+\delta) \cdot P^1_{dR} \tag{A.5g}$$
$$SOE^2_R(t+1) = SOE^2_R(t) + \frac{1}{E_R}(1-\delta) \cdot P^2_{cR} - \frac{1}{E_R}(1+\delta) \cdot P^2_{dR} \tag{A.5h}$$
$$SOE_R(x_{time}) - SOE^1_R(x_{time}) = 0 \tag{A.5i}$$
$$SOE_R(x_{time}) - SOE^2_{R(}x_{time}) = 0 \tag{A.5j}$$
$$P_{sell}(t) = \begin{cases} 0 \text{ for } t \in [x_{time}+1, \mathcal{T}] \\ \text{otherwise (A.5c)} \end{cases} \tag{A.5k}$$
$$P_{buy}(t) = \begin{cases} 0 \text{ for } t \in [x_{time}+1, \mathcal{T}] \\ \text{otherwise (A.5c)} \end{cases} \tag{A.5l}$$
$$P^s_{sell}(t) = \begin{cases} 0 \text{ for } s = 1,2, \quad t \in [1, x_{time}] \\ \text{otherwise (A.5d) / (A.5e)} \end{cases} \tag{A.5m}$$
$$P^s_{buy}(t) = \begin{cases} 0 \text{ for } s = 1,2, \quad t \in [1, x_{time}] \\ \text{otherwise (A.5d) / (A.5e).} \end{cases} \tag{A.5n}$$

A.2 Additional Results:

A.2.1 BEV arrival time in a LP setting

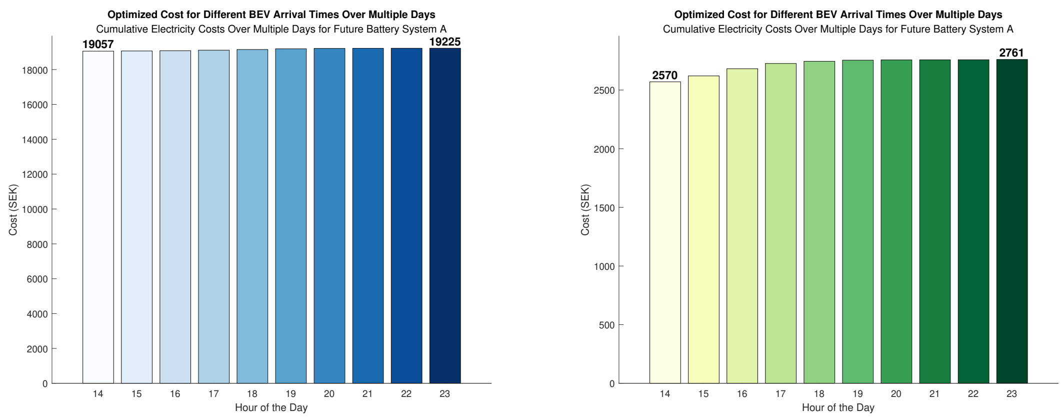

(a) Winter day

(b) Summer day

Figure A.1: Cost differences for various BEV arrival times on 100 winter days and 100 summer days for Future battery system A.

A.2.2 RESS/BEV Trajectories for three scenarios

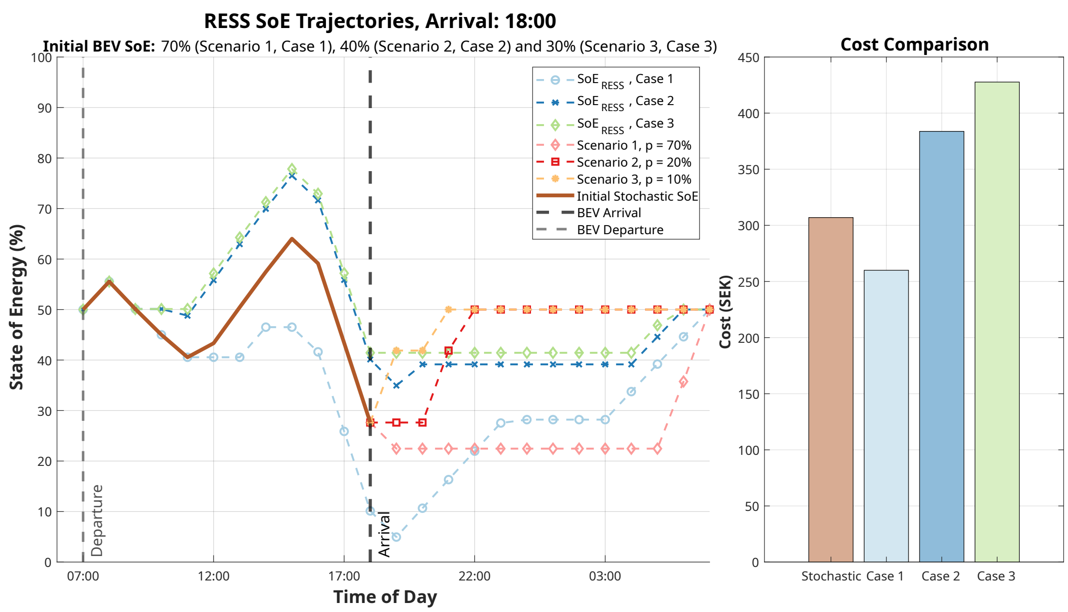

Figure A.2: SOE trajectories of the BEV on a winter day, with Future System B (100 kW). The BEV arrives at 18:00, with three possible scenarios.

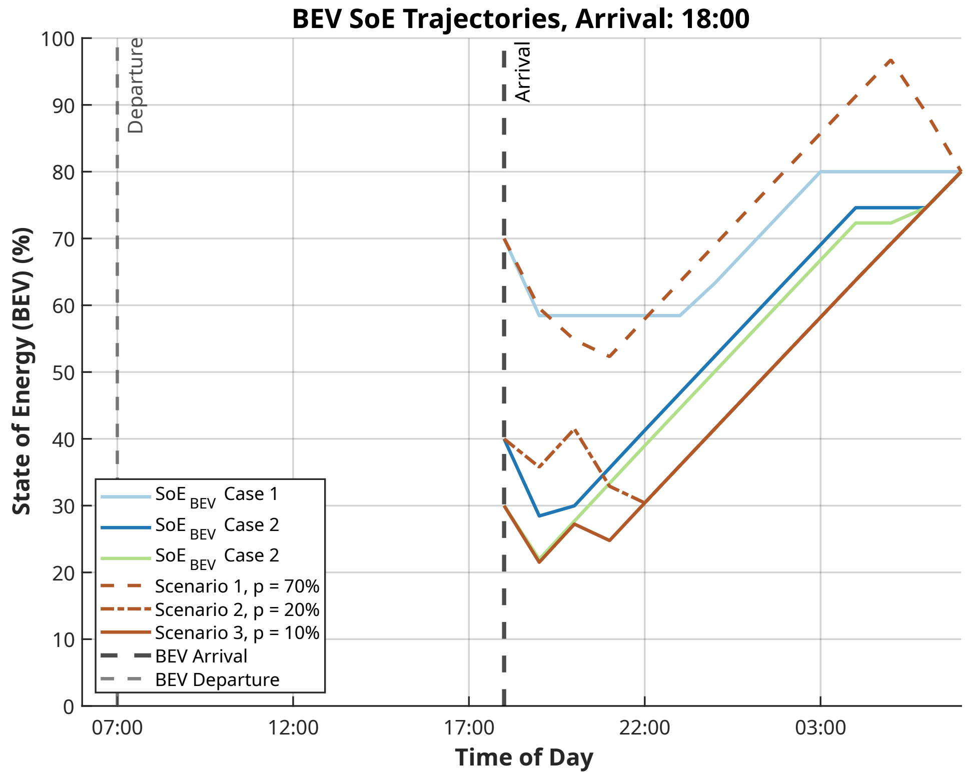

Figure A.3: SOE trajectories of the RESS and corresponding cost comparison for a winter day, using Future System B (100 kW). The BEV arrives at 18:00, with 3 possible scenarios.

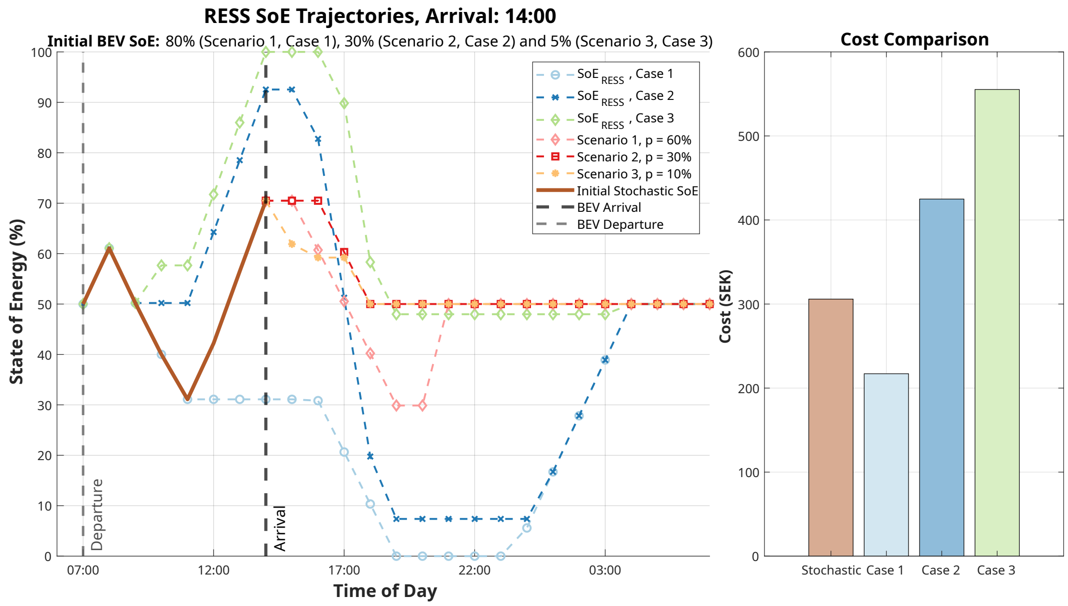

Figure A.4: SOE trajectories of the BEV on a winter day, with Future System A (50 kW). The BEV arrives at 14:00, with three possible scenarios.

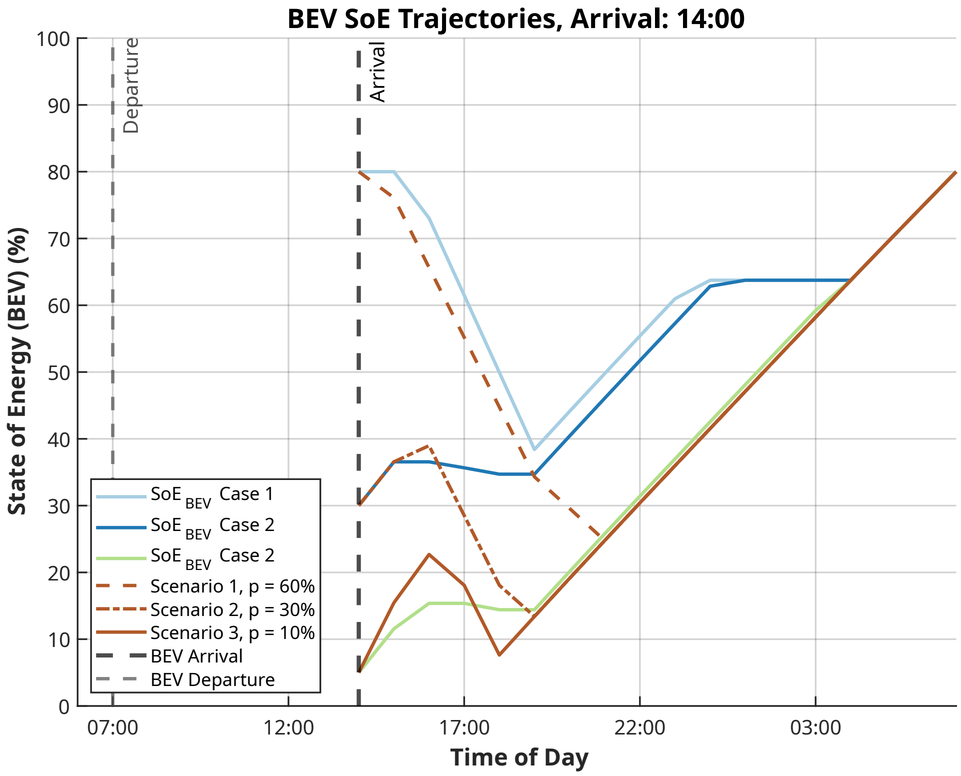

Figure A.5: SOE trajectories of the RESS and corresponding cost comparison for a winter day, using Future System A (50 kW). The BEV arrives at 14:00, with 3 possible scenarios.

DEPARTMENT OF SOME SUBJECT OR TECHNOLOGY
CHALMERS UNIVERSITY OF TECHNOLOGY
Gothenburg, Sweden
www.chalmers.se

AVANCEZ
1829
CHALMERS
UNIVERSITY OF TECHNOLOGY